

The University of Nottingham

UNITED KINGDOM · CHINA · MALAYSIA



UNIVERSITY OF BIRMINGHAM

Tackling antimicrobial resistance through two novel methods: repurposing vanoxerine as a novel anti-tubercular drug; and silencing virulence in Pseudomonas aeruginosa through inhibition of PqsR

A research report submitted by
Scott Grossman
under the supervision of Dr Luke Alderwick and Dr Michael Stocks

as part of the requirement for the degree of
MRes. Antimicrobials and Antimicrobial Resistance

Supported by wellcome trust

31st July 2018
Word Count 16916

Contents

Table of Contents

Contents ..... ***i***

Table of Contents ..... ***i***

Abstract ..... ***ii***

Acknowledgements ..... ***iii***

Abbreviations ..... ***iv***

1. Introduction ***1***

2. Vanoxerine: giving old drugs a new purpose for TB therapy ***9***

Abstract ***9***

Introduction **9**

Project basis **11**

Materials and methods **12**

Results and Discussion **16**

Conclusion **24**

3. Tackling antimicrobial resistance in Pseudomonas aeruginosa: exploring 6-chloro-3-(thiazol-4-ylmethyl)quinazolin-4(3H)-one derivatives as antagonists of PqsR ***25***

Abstract ***25***

Introduction **25**

Results and Discussion **28**

Conclusions **36**

4. Future works and concluding remarks ***37***

5. References ***40***

S1- Additional data for chapter 2 ..... ***44***

S2 – Experimental procedures for chapter 3 ..... ***48***

Abstract

The antimicrobial resistance crisis is one which will persist and worsen without intervention. This thesis looks to explore two innovative research areas in order to develop new antibiotics and stem the rise in antibiotic resistance. The first project looked at the potential to repurpose the former central nervous system (CNS) drug candidate vanoxerine into an anti-tubercular compound. Previous work has suggested that vanoxerine acts as a prodrug in mycobacteria and interacts with the monooxygenase enzymes Rv0565c and Rv3518c of *Mycobacterium tuberculosis* (*Mtb*). In this work a MIC_{50} assay was utilised to complete a structure-activity relationship (SAR) study and prove that vanoxerine is hydroxylated *in vivo* to its active form. Further to this, a global lipid analysis was completed suggesting that when treated with analogues of vanoxerine a lipid biosynthetic pathway was halted, though the lipid itself could not be identified. Although mass spectrometry was employed to identify changes in lipid concentrations at varying concentrations of drug, no trends were clear. However, the mass spectrometry data did indicate that analogues of vanoxerine were also hydroxylated *in vivo*, furthering the original hypothesis.

A further novel method for targeting antimicrobial resistance is the targeting of virulence systems. By inhibiting virulence but not affecting cell viability, no selection pressures are put on the pathogenic population. This enables the immune system to clear the infection without the host cells from being harmed by the release of toxins whilst preventing resistant subpopulations from dominating. In this work, a series of compounds were synthesised to act as antagonists to the protein PqsR, the autoinductive regulator of the quorum sensing system *pqs* in *Pseudomonas aeruginosa*. This system is associated with a range of effects including the synthesis of the toxin pyocyanin and the biofilm formation. Therefore, interference with these pathways may attenuate *P. aeruginosa* without encouraging selection of resistant bacteria. A biosensor reporter assay provided semiquantitative data suggesting that the majority of synthesised compounds reduced expression of the *pqs* system. Moreover, IC_{50} testing has been initiated, providing quantitative data on the potency of the synthesised series.

Acknowledgements

I would like to thank Dr Luke Alderwick and Dr Michael Stocks for both giving me the opportunity to work in their labs and providing me with guidance throughout. I would further like to thank everyone within their research groups who provided help and advice over the course of the year.

Abbreviations

6-APA	6-aminopenicillanic acid
A_2pm	*meso*-diaminopimelate
AHL	Acyl-homoserine lactone
Ala	alanine
AQ	alkyl quinolone
br	broad
CNS	central nervous system
Cy	cyclohexane
d	doublet
DCM	dichloromethane
DG	diacylglycerol
DMF	dimethylformamide
DMSO	dimethyl sulfoxide
FAME	fatty acid methyl ester
FDA	food and drug administration
Glu	glutamic acid
Gly	glycine
HATU	hexafluorophosphate azabenzotriazole tetramethyl uronium
HHQ	2-heptyl-4-hydroxyquinolone
HTS	high throughput screening
IC_{50}	half maximal inhibitory concentration
^{i}Pr	isopropyl
ITC	isothermal titration calorimetry
LC	liquid chromatography
MAME	mycolic acid methyl ester
MDR	multi-drug resistant
Me	methyl
MeOH	methanol
MIC	minimal inhibitory concentration
MPM	Mannosyl-beta1-phosphomycoketides

MRSA	methicillin resistant *Staphylococcus aureus*
MS	mass spectrometry
Mtb	*Mycobacterium tuberculosis*
NAG	*N*-acetylglucosamine
NAM	*N*-acetylmuramic acid
NBS	*N*-bromosuccinimide
NMP	*N*-methyl-2-pyrrolidine
NMR	nuclear magnetic resonance
OADC	Oleic Albumin Dextrose Catalase
OD	optical density
PBP	penicillin binding protein
PE	Diacylglycerolphosphoethanolamines
PG	Diacylglycerophosphoglycerols
Ph	phenyl
PI	Diacylglycerophosphoinositols
pqs	pseudomonas quorum sensing
PQS	pseudomonas quinolone signal
q	quartet
R_f	retention factor
s	singlet
SAR	structure-activity relationship
t	triplet
TB	tuberculosis
^{t}Bu	*tert*-butyl
TDM	Trehalose Dimycolates
THF	tetrahydrofuran
TLC	thin layer chromatography
TMM	Trehalose Monomycolates
XDR	extensively-drug resistant

1. Introduction

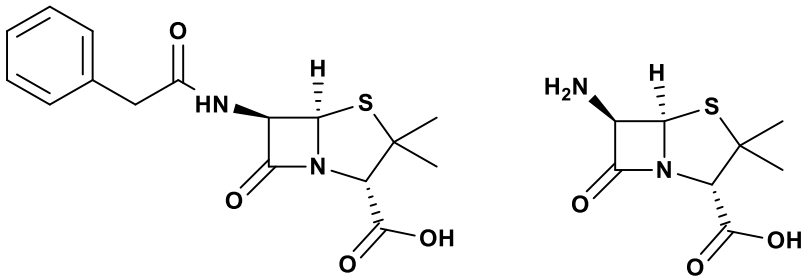
Ever since the discovery of penicillin by Alexander Fleming in 1928,[6] antibiotic resistance has been an ever-increasing problem. Antibiotics have become an essential commodity within society, curing previously fatal infections and providing protection for immunocompromised patients.[7] They have had a huge impact in increasing life expectancy, particularly through reducing infant mortality rates and have wide ranging fiscal impacts, significantly benefitting economies by improving the health of the workforce.

However, through a combination of misuse, overprescribing and natural evolutionary processes, resistance to every known antibiotic has been encountered. The spread of resistance has been exacerbated by patients failing to complete antibiotic courses and its use for non-medicinal purposes, such as in the farming industry where it is utilised as a growth hormone.[8-9] Whilst isolated cases of resistance are not of noteworthy concern, the rise of multidrug and extensively drug resistant bacteria hampers attempts to cure disease and has in the past nullified antibiotics to the extent that they are no longer valid treatment options, as in the case of methicillin.

The discovery of antibiotics

Penicillin marked a turning point in medicine: isolated from the fungus *Penicillium notatum*, it was the first naturally occurring antimicrobial and showed marked improvements over the few existing antimicrobials of the time, namely fewer side effects and an improved solubility. Following the discovery of a semi-synthetic route to penicillin *via* a 6-aminopenicillanic acid (6-APA) core (Figure 1.1),[10] syntheses of new penicillin derivatives were developed, leading to the production of drugs with broader spectra, fewer side effects and targeting strains of bacteria with specific resistance mechanisms.[11]

By 1960 a further eight classes of antimicrobial had been discovered, a mixture of natural products, such as aminoglycosides and glycopeptides,[12-13] as well the fully synthetic antimicrobial class of nitroimidazoles.[14] Although many drugs have become obsolete over time, the development of new generations of each class of drug enable resistance mechanisms to be tackled. In some cases, some of the earliest antibiotics developed are still used today: vancomycin, discovered in 1955, is one of the most important antibiotics currently used as it is capable of treating various drug-resistant pathogens such as MRSA.



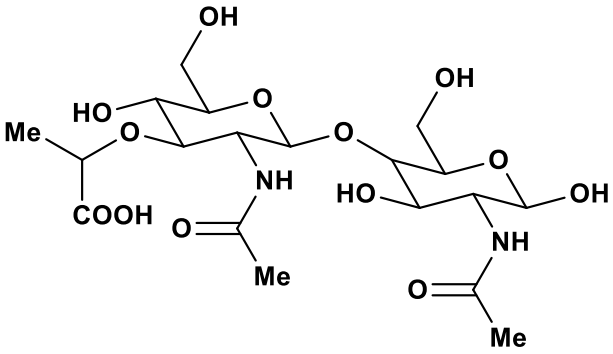
1. Penicillin G **2. 6-APA**

Figure 1.1 (left) The structure of the natural product penicillin G, extracted from the mould Penicillium notatum; (right) the structure of 6-APA, from which a variety of penicillins could be synthesised. 6-APA is fermented with acyl chlorides and sodium carbonate, forming an amide bond at the primary amine.

Mode of action

Each class of antibiotic has a unique mode of action against bacteria. They do all, however, target components of bacteria which are either unique to prokaryotes or are vastly different from mammalian cells. For example, penicillins act by interfering with cross-linking in the bacterial peptidoglycan, which strengthens the cell wall. Anti-tubercular drugs interfere with various processes in mycobacteria's intricate cell wall, and polymyxins ionically bond to negatively charged regions of the outer membrane in bacteria through the displacement of calcium and magnesium cations.

In the case of penicillin, cell lysis occurs through the competitive inhibition of transpeptidase enzymes which create cross-links between peptidoglycan layers. The polysaccharide spine of peptidoglycan consists of alternating sugars *N*-acetylglucosamine (NAG) and *N*-acetylmuramic acid (NAM) linked through a β-1,4 bond (Figure 1.2). Within this disaccharide subunit, the NAM is typically substituted at the D-lactyl group with a pentapeptide. Although there is much variation within this pentapeptide, a typical make-up would be L-Ala-D-Glu-*meso*-A_2pm-D-Ala-D-Ala.



3. A NAG-NAM subunit

Figure 1.2 The structure of a NAG-NAM subunit, which forms the peptidoglycan layers in many bacterial cell walls. Cross-linking occurs between the free carboxylic acid moieties of NAM saccharides (left) in adjacent peptidoglycan layers.

Transpeptidase enzymes, frequently known as penicillin binding proteins (PBP), bind the fourth and fifth residues of the pentapeptide, D-Ala-D-Ala, in their active site and cross-linking is achieved in two sequential half-reactions.[15] First the fifth residue, D-Ala, is cleaved in a serine-directed acylation reaction, followed by the cross-linking to another pentapeptide at the third residue, generally a diamino amino acid such as A_2pm or lysine, in a deacylation reaction. Gram positive bacteria typically incorporate interpeptide bridges, such as $(Gly)_5$, whereas Gram negative bacteria often directly cross-link the peptide chains (Figure 1.3).[16]

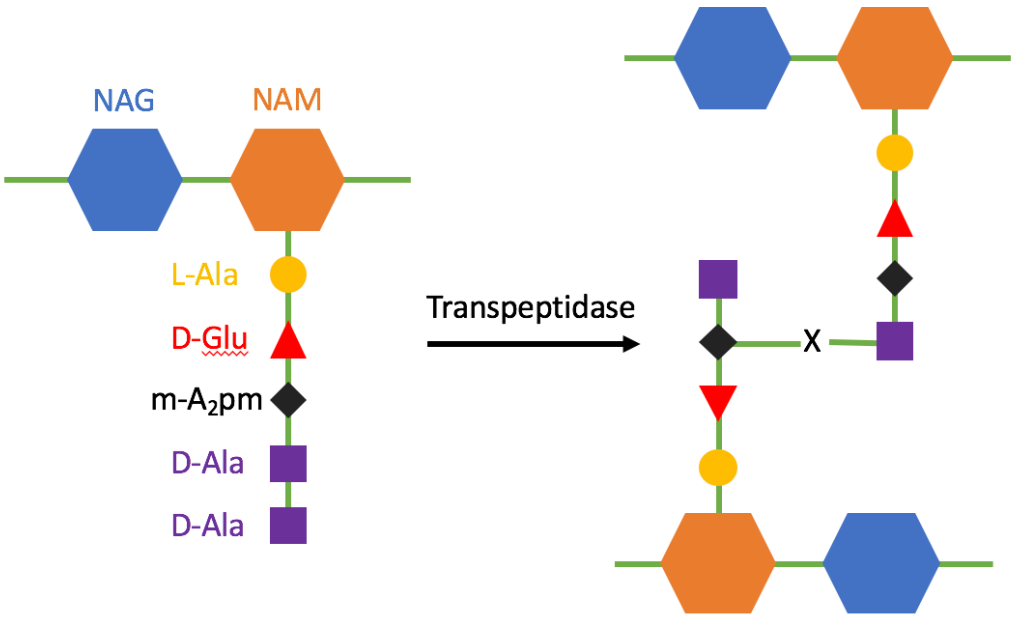


Figure 1.3 Transpeptidation of two peptidoglycan layers occurs over two steps: firstly the terminal D-Ala is cleaved by the transpeptidase enzyme, then a bond is formed between the remaining D-Ala unit and a nucleophile in a second peptidoglycan layer, such as is found in m-A_2pm. The bridge connecting the layers, represented by X, may be a single bond or may be more elaborate, such as a peptide bridge composed of $(Gly)_5$.

Penicillins can directly prevent this transpeptidation by occupying the active site of PBPs. The amino-β-lactam structure mimics the structure of D-Ala-D-Ala, so acts in place of peptidoglycan in the acylation half-reaction. However, having no second nucleophile capable of deacylating the PBP means that the covalent link between the enzyme and mimetic substrate is permanent, thus preventing any future transpeptidation by the enzyme.

Unsurprisingly, there are various other mechanisms by which antibiotics work, which target a variety of bacterial components. As mentioned previously the outer membrane is targeted by polymyxins,[17] protein synthesis is interrupted by various drugs such as linezolid,[18] gentamicin[19] and glycylcyclines,[20] and rifamycins and quinolones inhibit RNA and DNA synthesis.[21-22] Treatments for infections of resistant strains of bacteria frequently adopt a multidrug approach, whereby a variety of cellular components are targeted for higher efficacy.

Resistance mechanisms

The first widespread resistance mechanism noted was the appearance of β-lactamases. These are a class of secretory enzyme whose sole known purpose is the metabolism of β-lactam compounds. They are found more frequently in Gram negative bacteria, and as such act as the main defence system against penicillins in Gram negatives,[23] though are still common in Gram positives. Given a relatively strong homology between β-lactamases and PBPs, it is believed that β-lactamases may have directly evolved from a PBP, likely a DD-transpeptidase.[24] Unlike PBPs though, β-lactamases have no transpeptidase activity, but instead acylate β-lactam containing compounds, converting them into penicilloyl derivatives. These are then hydrolysed by water, thereby regenerating the β-lactamase enzyme. Half-lives for the β-lactamase-penicilloyl compound have been found to be six orders of magnitude lower than that of PBP-penicilloyl equivalents, since the latter is not deacylated by water. Hence, enzymatic activity of β-lactamases is a fast and effective method deployed by bacteria to resist penicillins.

Evolution has led to the production of a range of β-lactamases which have subsequently been classified into four groups, each with their own subgroups. Of these four groups, three demonstrate hydrolytic activity through a serine residue in the active site, acting as a nucleophile capable of attacking the β-lactam carbonyl (A, C, D). The remaining group (B) is a metalloenzyme with zinc atoms present in the active site (Figure 1.4).[25] It is believed that the zinc enables coordination of a hydroxide ion, which acts the nucleophile in place of the serine residue.[26]

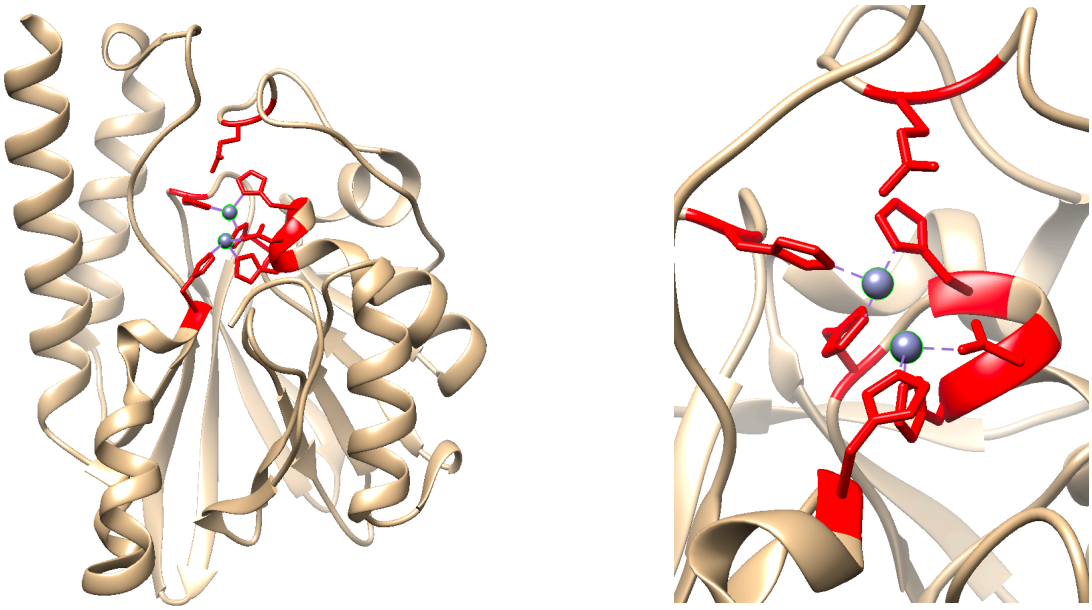
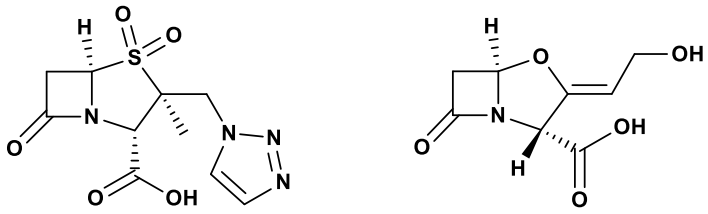


Figure 1.4 Structure of Serratia marcescens metallo-β-lactamase SMB-1. The active site (red) contains two zinc ions (purple) bound by coordinating residues, primarily histidines [adapted from Wachino et al., 2013].[1]

Increased use of antibiotics led to a dramatic increase in the occurrence of β-lactamases across the prokaryotic world. However, the development of several sacrificial compounds which could be co-administered with penicillins prevented the nullification of all penicillins which had already been developed. Most notably, clavulanic acid and tazobactam, both β-lactams themselves, went into clinical use (Figure 1.5). Clavulanic acid is most commonly prescribed alongside amoxicillin and is believed to deactivate β-lactamase by binding first to the serine in the active site, then following a rearrangement of the enzyme, it is attacked by a further nucleophile in the enzyme which inactivates the enzyme fully.[27] Since it binds specifically to a serine, it is incapable of inhibiting class B metalloenzymes. Tazobactam has been shown to have a variety of inactivation routes dependent on the class of β-lactamase encountered, but generally it is thought to be a reversible inhibition.[28] As tazobactam can act *via* several routes, it also shows some inhibition of class B β-lactamases. It is combined with piperacillin as a treatment of nosocomial *Pseudomonas aeruginosa*.



4. Tazobactam **5. Clavulanic acid**

Figure 1.6 Examples of two sacrificial compounds developed to prevent obsolescence in existing antibiotics. Tazobactam is used in conjunction with the drug piperacillin and clavulanic acid with amoxicillin.

Gram positive bacteria exhibit a different strategy as their primary defence: they utilise modified PBPs which still have transpeptidase activity, whilst also having a low affinity for penicillin substrates. The most notable modified PBP is PBP2a, which is the enzyme responsible for methicillin resistance in *Staphylococcus aureus* and a variety of other species through horizontal gene transfer (Figure 1.6). PBP2a does not replace any other transpeptidase in MRSA, but is simply synthesised in addition to the other transpeptidase enzymes.[29-30] PBP2a has a specifically low affinity to β-lactams due to modifications around the serine residue in the active site. Therefore it has a much lower rate of acylation than other PBPs.

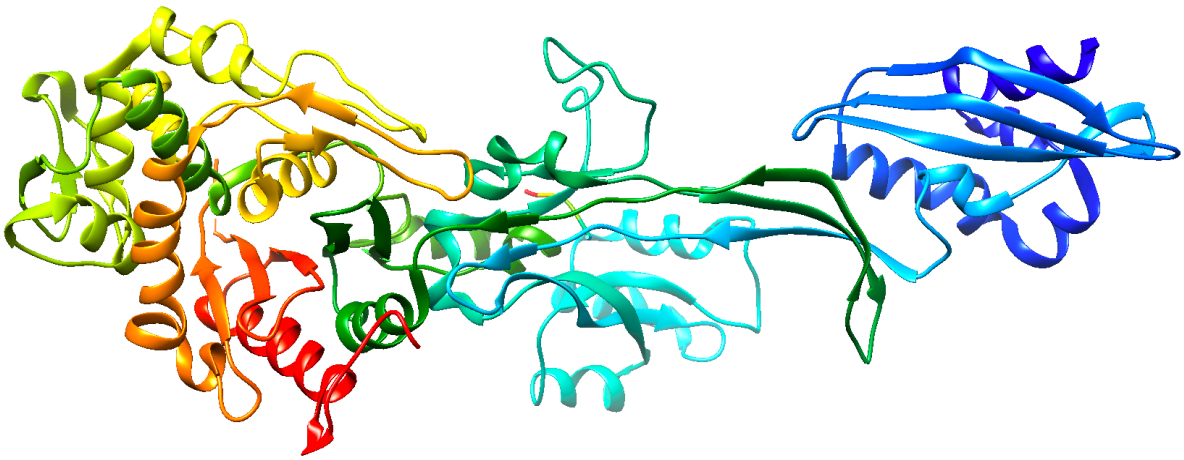


Figure 1.5 Ribbon structure representation of the MRSA transpeptidase PBP2a, which provides it with methicillin resistance [taken from Otero et al. 2013].[3]

One further example of a modified PBP is PBP5, found in *Enterococcus faecium*. This enzyme has a naturally low affinity for penicillins, but is still inhibited by them in many circumstances. However, overexpression of the enzyme and genetic modifications have been seen and both proven to confer resistance to the bacterium.[31] There are fewer methods of tackling modified PBPs in comparison to β-lactamases. The use of alternate drugs is the most common approach when resistance is widespread, as shown by the obsoleteness of methicillin following the spread of methicillin resistance. As such, modified PBPs have the potential to ravage options when it comes to dealing with multi-resistant bacteria.

Novel methods targeting AMR

Ever since the discovery of penicillin, bacteria have counteracted the progress of antibiotics with the development of resistance mechanisms. The rate of resistance is rising faster than the rate of development of new antibiotics from traditional discovery methods. As such, it is important to develop novel antimicrobials capable of evading existing antimicrobial mechanisms or alternatively, develop antimicrobials in a much quicker timeframe.

One suggested method is to target microbial virulence without affecting cell viability.[32] It is hypothesised that in doing so, no selection pressures will be exerted on the pathogenic population, but the bacteria will be rendered harmless. Therefore, the immune system can clear the body of pathogens which are incapable of resisting attack. One example is the targeting of quorum sensing systems, whereby through preventing quorum sensing, the production of toxins and biofilms is suppressed. This both prevents the host cells from being damaged or killed, and also prevents the invading population from mobilising a defence. Theory suggests that through this method resistance to drugs targeting quorum sensing should not be a major issue when compared against traditional approaches due to a lack of selection pressure.

Further to novel discovery methods, a faster pipeline is required to develop drugs targeting pathogens with higher rates of resistance and those where resistance is rising rapidly. One such target is tuberculosis (TB), caused by *Mycobacterium tuberculosis* (*Mtb*). Cases of multi-drug resistant and extensively-drug resistant infections are increasing annually and given TB's persistence generally, it is very difficult to treat. A method that has been adopted to target this problem is drug repurposing, through which previously FDA approved drugs are recycled for a different purpose. This means that the first stages of drug development can be passed over, having already been tested previously, and testing can be moved on immediately to clinical trials after confirming efficacy against the target.

This work looks to explore these two methods as a method of combatting microbial resistance. Chapter Two will discuss research looking at vanoxerine, a drug trialled as a cocaine addiction treatment. Recent research has shown it to display antitubercular activity, and as such is a candidate for drug repurposing. A SAR study was conducted to prove a theory that it acts as a pro-drug and is hydroxylated to its active form, which interferes with lipid synthesis. Further

to this, lipid analyses were conducted in conjunction with mass spectrometric analysis to develop this theory.

Chapter Three discusses the synthesis of a novel hit compound targeting the quorum sensing system *pqs* in *P. aeruginosa*. This system contains several potential drug targets, but focus was placed on PqsR, the autoinductive regulator which is key to the production of the natural agonist, PQS. It has been postulated that disruption of this system may reduce both toxin production and biofilm formation. In this work, a comprehensive SAR study provided a range of compounds which were subsequently tested *via* a biosensor reporter assay and IC_{50} assays.

2. Vanoxerine: giving old drugs a new purpose for TB therapy

Abstract

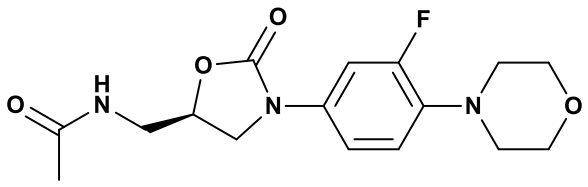
In an effort to tackle the rising problem of multidrug-resistant and extensively-drug resistant tuberculosis, drug repurposing has become an important tool in the search for new antibiotics. Herein we report that vanoxerine, a former cocaine addiction treatment candidate, shows potential for repurposing given newly found antimycobacterial properties. A structure-activity relationship study of vanoxerine and a range of derivatives *via* a MIC_{50} assay showed a ring with an unfunctionalised *para*- or γ-position to be vital. Both aliphatic and aromatic rings displayed activity. Moreover, a global lipid analysis provided indications as to the effects the drugs were having on cell wall biosynthesis. When combined, the MIC_{50} assay and global lipid analysis bolstered the belief that vanoxerine is a pro-drug activated *in vivo* through hydroxylation at the *para* site of the phenyl ring. Additionally, subcloning of the gene MSMEG_2240, a monooxygenase believed to activate vanoxerine, into *Escherichia coli* BL21(DE3) and *E. coli* T7 shuffle has laid a foundation for future enzyme expression and purification, to enable further studies.

Introduction

Mycobacterium tuberculosis (*Mtb*), the causative agent of tuberculosis (TB) in humans, infects one third of the world's population and killed approximately 1.7 million people in 2016 according to a World Health Organisation report.[33] It is currently the world's leading cause of death from infection and although the mortality rate has decreased since 2000, cases of multidrug-resistant (MDR) and extensively-drug resistant (XDR) TB are increasing, meaning new treatment options are of high importance. Rates of MDR-TB vary throughout the world, but reached levels of 13.1% across Europe in 2010-2011 amongst previously untreated TB cases. Levels rose to 44.2% amongst previously treated TB cases.[34] Similar trends are seen worldwide, such as in KwaZulu-Natal in South Africa, where the first cases of XDR-TB were reported, rates averaged 10% in newly diagnosed cases and 32% in those treated previously for TB from 2007-2009.[35]

Repurposing old drugs for new targets is a desirable method for the development of new antimicrobials as it eliminates the need to progress through all stages of clinical trials, thus saving both time and money.[36-37] Therefore, it is a particularly suitable method for combatting MDR and XDR bacterial strains where speed is imperative to counter rises in resistance. Various drugs have been repurposed previously, particularly in searching for new second-line treatments to TB, of which linezolid is a prime example. In combination with other antimicrobials linezolid, previously used to treat MDR Gram-positive infections, was found to effectively treat MDR-TB (Figure 2.1).[38] As such drug repurposing is a proven method of targeting TB with the potential of stemming the rise in MDR and XDR cases.

Targeting cell wall synthesis is one of the key focusses of TB treatments; *Mtb* has a unique cell wall structure which is notably much thicker and as a result more difficult to penetrate than most other bacteria. Its complexity and size are key to the bacterium's ability to persist and resist external threats such as immune systems and high osmotic pressures and overall makes TB one of the most difficult to treat bacterial conditions. Currently, treatment of latent TB with first-line medication takes three months and treatment for active pulmonary TB takes six months due to the bacterium's ability to resist antibiotics. Key features of the *Mtb* cell wall include mycolic acids, arabinogalactan and a cross-linked peptidoglycan.[39-40] Importantly, there is a high proportion of lipid-based compounds in the cell wall including glycerolipids, glycerophospholipids and many of the mycolic acids themselves are fatty acyl chains. Therefore, targeting lipid production is an effective method to disrupt cell wall biosynthesis and could benefit the development of novel therapeutics.



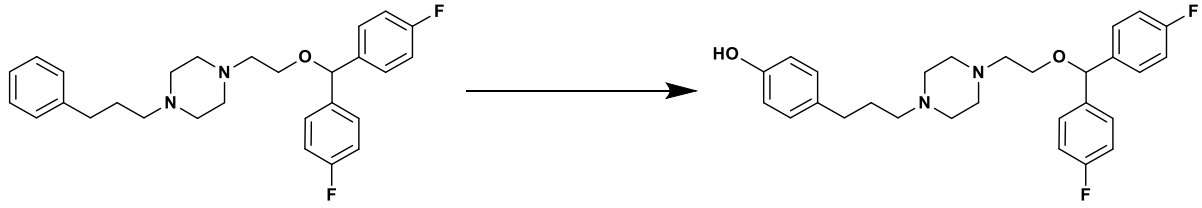
6. Linezolid

Figure 0.1 The structure of linezolid, which was originally designed as a broad spectrum antibiotic capable of treating antibiotic resistant skin infections and pneumonia, and was successfully repurposed to further treat drug-resistant cases of TB

Project basis

Previous research at the University of Birmingham (unpublished) utilised high throughput screening (HTS) to identify possible existing drugs as new antimycobacterials, in which vanoxerine was identified as a hit against *Mtb*. Vanoxerine was initially developed as a treatment to the neurodegenerative disease Parkinson's, but was found to have little efficacy. Alternatively, research was undertaken looking into the possibility of treating cocaine addiction and heart arrhythmias, but efforts were stopped before phase III trials due to safety concerns specifically within the treatment of cocaine addiction.[41-42] However, following on from the HTS, there is an opportunity to explore vanoxerine's potential as an antimicrobial instead of a central nervous system (CNS) drug.

Previously, vanoxerine resistant mutants were grown by culturing *Mycobacterium smegmatis* in high concentrations of vanoxerine, a mycobacterial strain frequently used as a model for *Mtb* due to its relatively fast growth rate. Non-synonymous mutations were found in the genes MSMEG_2038 and MSMEG_2240. These correspond to Rv0565c and Rv3518c respectively in *Mtb*, which are both believed to have monooxygenase activity. The former is a putative flavin-binding monooxygenase and the latter a putative cytochrome P450 enzyme. Although initially believed to be the target of vanoxerine activity, further work suggested that these monooxygenases activated vanoxerine *in vivo* to its potent, *para*-hydroxylated form (unpublished, Scheme 2.1).



7. **8.**

*Scheme 0.1 The suspected in vivo hydroxylation of vanoxerine (**7**) to compound **8** is hypothesised to activate the compound giving it antimycobacterial properties.*

Monooxygenases are believed to be vitally important to *Mtb*, particularly throughout its dormant life within a macrophage. Mycobacteria are able to sustain all of their carbon needs living solely off of cholesterol, but further to this it has been suggested that certain monooxygenases may also contribute to cell wall biosynthesis,[43] such as in the biosynthesis of lipids and glycolipids. The interconnectedness of these two processes suggests that if the monooxygenases' direct enzymatic activity was not the target of vanoxerine, then it is possible that cell wall biosynthesis is a target; as a substrate of Rv0565c or Rv3518c (Figure 2.2) or

both, it is possible that its active structure may interfere with a route to lipid production, should either of these enzymes be involved in the process of cell wall biosynthesis.

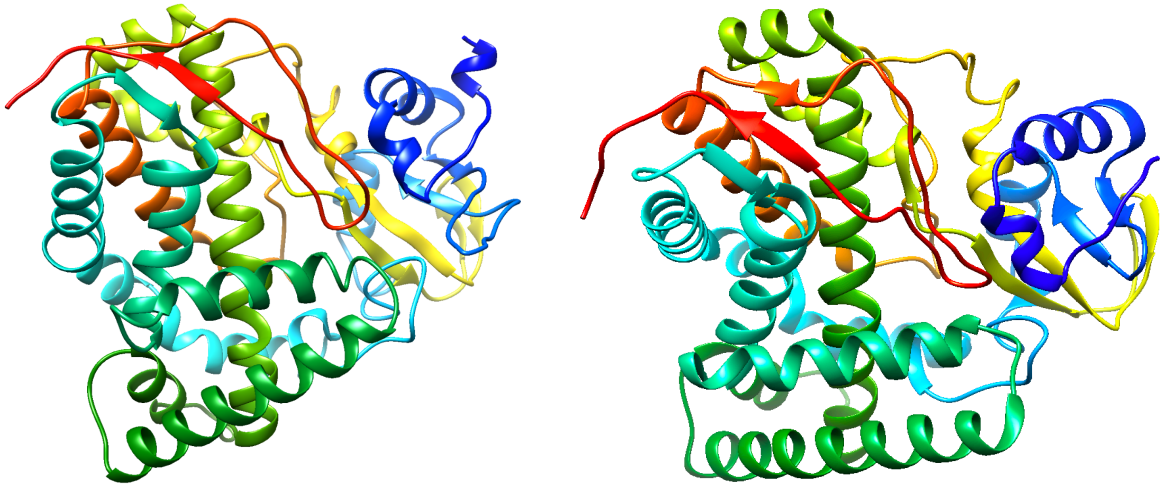


Figure 0.2 (Left) predictive structure of MSMEG_2240, a putative cytochrome P450 enzyme based on iTASSER model; (right) comparative structure of Rv3518c, cyp 142, whose crystal structure (PDB = 2XKR)[2] was used as a base model for the iTASSER modelling

On the basis of this previous research, we hypothesise that vanoxerine's activity is based on its ability to inhibit cell wall biosynthesis. Herein we provide evidence in the way of MIC_{50} testing to propagate the theory of *in vivo* activation of vanoxerine *via* hydroxylation by a monooxygenase. Furthermore, a global lipid analysis offers preliminary data on the effects of vanoxerine derivatives on cell wall composition. Finally, subcloning of an overexpressor plasmid of MSMEG_2240 into *E. coli* was completed as a platform for future attempts to synthesise and purify the enzyme.

Materials and methods

List of strains

Strain	**Features**	**Reference**
M. smegmatis MC^2 155	Wild-type *M. smegmatis*	[44]
M. bovis BCG	Wild-type *M. bovis* BCG	[45]
E. coli TOP10	Electrocompetent *E. coli*	[46]
E. coli BL21(DE3)	Plasmid expression strain of *E. coli*	[47]

E. coli T7 shuffle	Plasmid expression strain of *E. coli*	[48]
Plasmid	**Description**	**Origin**
pVV16_2038	pVV16 plasmid containing gene MSMEG_2038 under the control of a constitutively expressed promoter. Kan^R.	Unpublished. Christopher Burke (University of Birmingham)
pVV16_2240	pVV16 plasmid containing gene MSMEG_2240 under the control of a constitutively expressed promoter. Kan^R	Unpublished. Christopher Burke (University of Birmingham)

Culturing *M. smegmatis*

M. smegmatis was cultured in Middlebrook 7H9 broth with 0.5% glycerol and 0.25% tween 80. Liquid cultures were incubated at 37 ºC with shaking at 220 rpm. No antibiotic markers were required for the strains used. Cultures were passaged every three days up to a maximum of four times, following which a new colony was picked from an agar plate.

Culturing *M. bovis* BCG

M. bovis BCG was cultured in Middlebrook 7H9 broth with 10% OADC and 0.25% tween 80. Liquid cultures were incubated at 37 ºC with 5% CO_2. No antibiotic markers were required for the strains used. Cultures were passaged every seven days up to a maximum of four times, following which a new colony was grown from a glycerol stock.

Culturing *E. coli* strains

E. coli was cultured in LB broth with antibiotic marker. Hygromycin B, kanamycin and ampicillin were used at 150 μg mL^{-1}, 50 μg mL^{-1} and 100 μg mL^{-1} respectively. Liquid cultures were incubated at 37 ºC with shaking at 220 rpm.

Broth dilution MIC_{50} assay for *M. smegmatis* and *M. bovis* BCG

96-well flat-bottom plates were filled with 100 μL Middlebrook 7H9 broth containing 0.25% tween 80 and 4% DMSO (*M. smegmatis*) or Middlebrook 7H9 broth containing 0.25% tween 80, 4% DMSO and 10% OADC (*M. bovis* BCG), from column two to 12. DMSO was added to aid in the solvation of compounds. Column one was filled with 200 μL of the same broth mixture, and either 8 μL drug (10 mM stocks) or 4 μL drug (20 mM stocks). A serial dilution from column two to 10 gave the desired concentration range of 200 μM to 38 nM. Each drug was tested in triplicate. Cells were grown to a mid-log value (OD_{600} = 0.4-0.8) and diluted in broth with 0.25% tween 80 (*M. smegmatis*) or 0.25% tween 80 and 10% OADC (*M. bovis* BCG) to OD_{600} = 0.1. 100 μL of said broth was added to each well in column one to 10 giving a final OD_{600} of 0.05. 100 μL of diluted cells were also added to column 12 as a positive control, and 100 μL of broth with 0.25% tween 80 (*M. smegmatis*), or 0.25% tween 80 and 10% OADC (*M. bovis* BCG), to column 11 as the negative control. Plates were incubated at 37 °C for 18 hours (*M. smegmatis*) or 37 °C with 5% CO_2 for seven days (*M. bovis* BCG), after which 40 μL of 0.02% resazurin in dH_2O was added to each well. The plates were incubated under the same conditions for a further six hours (*M. smegmatis*) or 24 hours (*M. bovis* BCG). An amplex-red endpoint assay was accomplished on a plate reader, exciting fluorescence at 530 nm and measuring emission at 590 nm. Living cells are able to metabolise resazurin into resorufin, causing a colour change from blue to pink, whereas resazurin remains blue in dead cells. Raw values were converted to % survival based on the mean values of the controls, where:

$$\%\ survival = \frac{raw\ value - mean\ of\ negative\ control}{mean\ of\ positive\ control - mean\ of\ negative\ control} \times 100\%$$

Global lipid extraction

M. smegmatis wild type was grown to OD_{600} = 0.5 and drug was added to test tubes containing 5 mL of culture at 0x, 0.5x, 1x, 2.5x and 5x the MIC_{50} of each drug **3**, **13** and **16** (MIC_{50} values were 24.60 μM, 97.56 μM and 94.88 μM respectively). Cultures were incubated at 37 °C with shaking at 220 rpm for 12 hours, before centrifugation for 10 minutes at 3000 g. Supernatant was removed and 2 mL of a solution of $CHCl_3$/MeOH/dH_2O (10:10:3) was added to each pellet. The resulting biphase was treated with 1 mL $CHCl_3$/MeOH (1:1) to form a single phase. The

solutions were then heated at 50 °C for two hours, before centrifugation at 3000 *g* for 15 minutes. The supernatant was transferred to a fresh tube and treated with 1.75 mL $CHCl_3$ and 0.75 mL dH_2O before vortexing and rotating to give a biphase. To dissolve any precipitate at the interface of the biphase, 0.1 mL of 5 M NaCl was added before vortexing and rotating again. The organic layer was transferred to a fresh tube and treated with 2 mL $CHCl_3$/MeOH/dH_2O (3:47:48) before vortexing for one minute and rotating for two minutes. The supernatant was removed and the pellet washed twice more with the $CHCl_3$/MeOH/dH_2O (3:47:48) solution. The organic phase was transferred to a fresh tube and dried at 50 °C. 1-D TLCs were run in $CHCl_3$/MeOH/dH_2O (60:16:2), $CHCl_3$/MeOH/dH_2O (80:20:2) and $CHCl_3$/MeOH/NH_4OH (80:20:2). All were stained in phosphomolybdic acid and $CHCl_3$/MeOH/dH_2O (60:16:2) was additionally stained in α-naphthol to visualise sugar-containing compounds.

Subcloning of MSMEG_2240 and MSMEG_2038

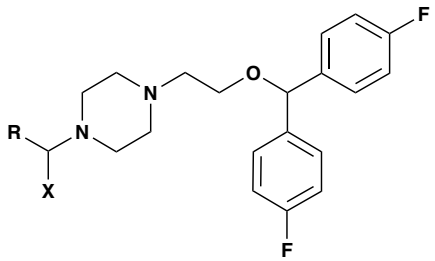
Vectors pVV16_2240 and pVV16_2038 were digested at the HindIII and NdeI sites yielding the genes MSMEG_2240 and MSMEG_2038, as visualised by 1% agarose gel. MSMEG_2240 was then ligated into pET23b using T4 DNA ligase, with incubation for one hour at room temperature. This was incubated with *E. coli* on ice for 20 minutes, before heat shocking at 42 °C for 30 seconds and a further incubation on ice for five minutes. To this, 250 μL LB broth was added and incubated at 37 °C for one hour before plating onto ampicillin containing LB agar. Empty vectors were also plated onto ampicillin containing plates, as well as fully transformed cells being plated onto agar containing no antibiotics as further controls. Plates were incubated at 37 °C for two days and successful transformants refrigerated. The same protocol was attempted for MSMEG_2038, but failed to yield the desired transformant.

pET23b_2240 was cultured overnight in LB broth containing ampicillin, following which the plasmid was harvested *via* plasmid miniprep. To ensure successful transformation, a double digest with HindIII and NdeI was completed, with results visualised on a 1% agarose gel proving the successful insertion of gene MSMEG_2240. The pET23b plasmid was then heat shocked at 42 °C using the same protocol as previously used in order to transform into *E. coli* BL21(DE3) and *E. coli* T7 shuffle, both of which are suitable strains for plasmid protein expression.

Results and Discussion

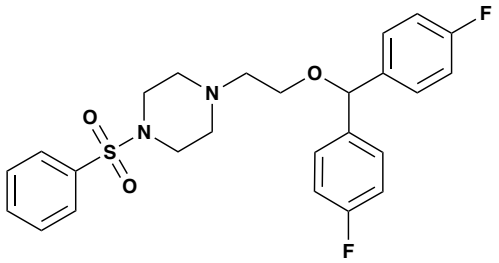
MIC_{50} testing of vanoxerine derivatives

To probe the theory of *in vivo* hydroxylation, MIC_{50} testing was completed on a range of vanoxerine derivatives. The structure-activity relationship was examined by testing compounds with a range of carbon linkers varied in length, the addition of heteroatoms and through functionalisation and branching, as well as by varying the functional group at the end of the carbon linker (Figure 2.3). The right-hand side of all derivatives was left unchanged, so as to focus our investigation on the properties of the unfunctionalised phenyl ring of vanoxerine specifically. However, current research is examining the effects of removing one aromatic ring from the right-hand side (unpublished).

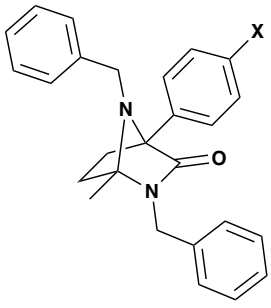


9. X = H, R = C_2H_4Ph
10. X = =O, R = O^tBu
11. X = H, R = Ph
12. X = H, R = CH_2Ph
13. X = =O, R = OCH_2Ph
14. X = H, R = $CH_2C(=O)Ph$
15. X = H, R = *p*-PhF
16. X = H, R = *p*-PhOH

17. X = H, R = Cy
18. X = =O, R = Ph
19. X = H, R = *p*-PhOMe
20. X = H, R = 3-pyridine
21. X = H, R = 3-indole
22. X = Me, R = Me
23. X = H, R = ^iPr
24. X = H, R = C_2H_4-*p*-PhOH



25.



26. X = H
27. X = Br
28. X = OMe

*Figure 0.3 The range of structures developed for the SAR study predominantly varied in length and terminal moiety of the linker (R) and functionalisation of the α-carbon of the linker (X). Compound **25** was designed to test linkers which were not carbon based, and hence a sulfoxide linker was used, and compounds **26-28** utilised a scaffold with a much more three-dimensional shape.*

It was expected that of the tested compounds, those with a chain length of three carbons would be the most potent, whilst requiring an aromatic ring with an unfunctionalised *para*-position to maintain activity. This describes the general structure of vanoxerine. Therefore, those with shortened chains or functionalised phenyl rings would be expected to be less efficacious. The effect of functionalisation or addition of heteroatoms to the ring were both expected to reduce potency due to altered electrostatic interactions with the unelucidated target. In total, 20 compounds were tested against *M. smegmatis* wild type and vanoxerine resistant mutants, and *M. bovis* BCG wild type. Four independently grown vanoxerine mutants were tested. Of the 20 compounds, 17 were vanoxerine analogues and three were 2,7-diazabicyclo[2.2.1]heptan-3-one derivatives.

Several key observations were made from the MIC_{50} assay. Most notably, structures with *para*-functionalised aromatics showed no activity. The only exception to this was compound **24**, which was *para*-hydroxylated and showed inhibition with MIC_{50} = 94.88 μM (wild type *M. smegmatis*, Figure 2.4). Compounds **15** and **19** which had *para*-functionalisations –F and –OMe respectively, showed no activity against any tested strains. This gives weight to the theory that *para*-hydroxylation activates vanoxerine to inhibit mycobacterial growth. Compound **16** was also *para*-hydroxylated, but showed no activity, identifying chain length as a key component of the molecule: compounds **24** and **16** differ only in the carbon linker length, with the longer chain giving activity below 200 μM, but the shorter showing no activity at such concentrations. This direct comparison suggests that a longer chain length aids in substrate binding.

This is yet to be fully qualified however, as other active compounds inhibited mycobacterial growth with a linker of one carbon. Both compounds **11** and **17** contained a shortened chain, whilst also retaining an unfunctionalised position *para* to the linker. These compounds displayed MIC values lower than that of **24**, with MIC_{50} = 24.60 μM and 24.25 μM respectively. In addition, it was observed that the addition of heteroatoms and functional groups had a negative effect on growth inhibition. No compounds with heteroatoms or functionalised chains showed any antimycobacterial properties as was initially predicted. The final compound to successfully demonstrate mycobacterial growth inhibition was **21**, though at the relatively higher concentration of MIC_{50} = 97.56 μM when compared with **11** and **17**. MIC_{50} values in

vanoxerine resistant *M. smegmatis* and wild type *M. bovis* BCG were comparable. The same trends were seen in all strains for all tested compounds (see S1).

Of all other compounds tested, no mycobacterial growth inhibition was seen, inclusive of the 2,7-diazabicyclo[2.2.1]heptan-3-one compounds tested. Curiously, compound **9**, lab synthesised vanoxerine, failed to show inhibition up to 200 μM throughout these experiments in all strains tested. Previous work (unpublished) showed lab synthesised vanoxerine to be far less potent than industrially produced vanoxerine, concurrent with the results displayed here.

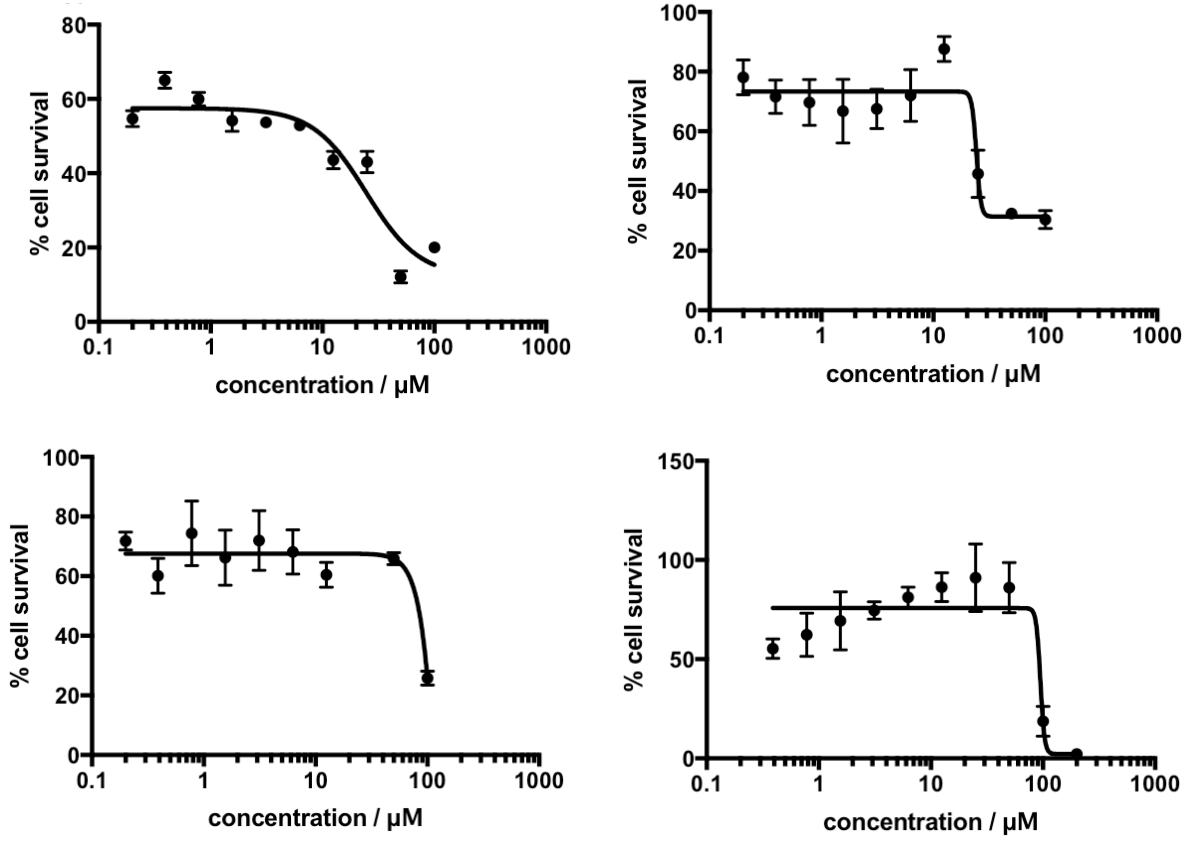


*Figure 0.4 MIC_{50} survival plots for compounds **11**, **17**, **24** and **21** (top left clockwise). Of these **11** and **17** were the most potent, with MIC_{50} values of 24.60 and 24.25 μM (top left and right respectively). Compounds **24** and **31** exhibited sub-100 μM IC_{50} values with 94.88 and 97.56 μM (bottom left and right respectively).*

Global lipid analysis

In order to investigate the derivative drugs' effects on the cell wall, lipid analyses were undertaken to study the changes in composition of various lipids in wild type *M. smegmatis* with increasing concentrations of drug. As an initial probe, a global 10:10:3 $CHCl_3$/MeOH/dH_2O extraction methodology was adopted, as it was not clear which, if any,

particular lipids would be affected by treatment of *M. smegmatis* with active compounds. Analyses were carried out with compounds **11**, **21** and **24**, but experiments with **17** were not possible due to limited stocks of the chemical. Following this an analysis of fatty acid methyl esters (FAMEs) and mycolic acid methyl esters (MAMEs) was undertaken.

Extractions were completed with concentrations of each compound varying from 0-5x the MIC_{50} value in order to give an overall indication as to the changes occurring in the concentrations of each lipid. Qualifications of these changes were recognised by thin layer chromatography (TLC). As the concentration of each drug was increased, the majority of lipids saw a decrease in spot intensity. This was expected, as once the concentrations exceed that of the MIC_{50} values cells begin to die. Two notable exceptions were observed though: in both compound **21** and **24** two molecules were seen to be increasing in concentration as the drug concentration increased, as visualised by TLC. One of these spots could be attributed to the drug itself (R_f = 0.59 and R_f = 0.69 for compounds **21** and **24** respectively in 80:20:2 $CHCl_3$/MeOH/dH_2O, Figure 2.5), whilst the second remained an unknown compound (R_f = 0.83 in 80:20:2 $CHCl_3$/MeOH/dH_2O).

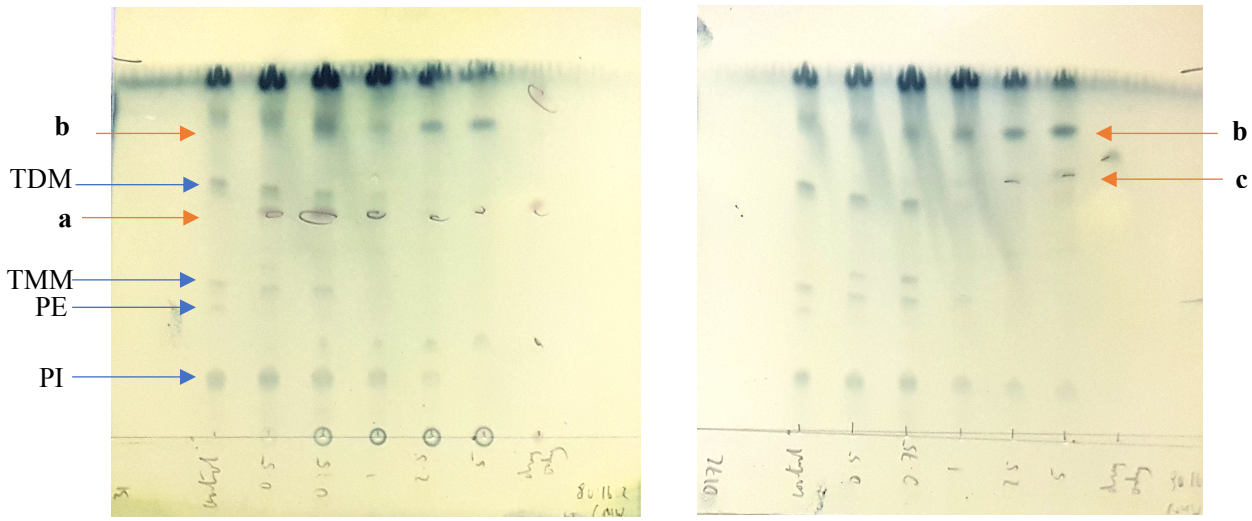


*Figure 0.5 TLCs of compounds **21** (left) and **24** (right), run in 80:20:2 $CHCl_3$/MeOH/dH_2O and stained in polymolybdic acid. The majority of observed lipids are seen to decrease in concentration as drug concentration increases. Concentrations of 0, 0.5, 0.75, 1, 2.5 and 5x the MIC_{50} value were run (lanes left to right) and only two spots were seen to increase in intensity as drug concentration increased. Spots **a** and **c** were characterised as the activated drugs by mass spectrometry, and both were visible under UV lamps. Compound **b** was believed to be a lipid in a biosynthetic pathway which was interrupted, but the exact structure could not be identified. Labelled spots PI, PE, TMM and TDM are diacylglycerophosphoinositols, diacylglycerolphosphoethanolamines, trehalose monomycolates and trehalose dimycolates respectively as compared against Bansal-Mutalik and Nikaido[4] and are integral components of the mycobacterial cell wall.*

It is possible that this unidentified compound is an intermediate lipid in a larger biosynthetic pathway, in which vanoxerine and its derivatives may interfere, hence causing an accumulation of this intermediate. It had also been hoped that a further spot of increasing concentration in the TLC of **21** may be seen, attributed to a hydroxylated form of it, but this was not observed. To explore the results of the lipid analysis further, mass spectrometry was employed to evaluate the TLC data more quantitatively.

Compound **11** was not found to show the same trends as **24** and **21**. Although more potent than both other compounds tested, no lipids were seen to increase in concentration upon treatment with it. Instead, concentrations remained largely constant, and **11** itself could not be clearly visualised. It is possible that compound **11** inhibits cell growth through an alternate pathway, which may explain its unexpected activity with just a one carbon chain. However, this would require further experimentation. Analysis of the MAMEs and FAMEs showed no clear trends in lipid concentration for any of the three compounds (S1).

Mass spectrometric analysis

In order to further evaluate the global lipid analysis experiments, mass spectrometry was performed on the samples. Initially, TLC-MS was adopted, whereby the sampling of spots directly from a TLC plate could indicate which lipids were present and where they could be located on the TLC plate. However, given the relatively low resolution of the instrument, few insights could be made. Having tested compounds **24** and **21**, both drugs could be identified as one of the spots of increasing concentration as had already been suggested. The other spot of increasing concentration could be seen to have more activity than all other tested spots, but none of the compounds present could be identified. Given more time, preparative TLCs would have been prepared, meaning spots could be scratched off and sent for higher resolution forms of mass spectrometry, whilst maintaining the specificity of the compounds sent for analysis.

However, samples of the extracted lipids were sent for LC-MS prior to separation with TLC at 0x, 1x and 5x the MIC_{50} value of each compound providing data on the changes in lipid concentrations as drug concentrations increase. The spectra showed clearly that the drugs **24** and **21** were seen in their unaltered forms, but furthermore a peak at m/z = 476.22 in the ESI-spectrum for compound **21** (1x MIC) corresponded to the $[M-H]^-$ peak of its hydroxylated

form, showing that *in vivo* hydroxylation is occurring. However, poor resolution of the spectra for **21** at 5x MIC meant that this could not be confirmed, though repeats will verify this. To further this finding, a mass corresponding to the hydroxylated form of **11** was found on its 5x MIC spectrum; although it was not clearly visible on the spectrum itself, the intensity at m/z = 439.22 was 4.46×10^6, 100x the average intensity for the given dataset. No other observations could be made directly from the spectra, but analysis of trends yielded potential leads with regards to affected lipids.

Although the raw dataset was of a daunting size, an attempt was made to observe some trends across the increasing concentrations of drug without the use of chemoinformatic software. Initially, datasets were filtered to only contain data points which corresponded with hits found on Lipid Maps® mycobacterial search tool and that were statistically significant (intensity threshold = 2000, mass tolerance = +/- 0.05 ppm, ion = $[M+H]^+$ or $[M-H]^-$, Δ/mass $\leq$ 5 ppm). From the remaining data, lipids were recorded where the intensity was seen to increase from 0x to 1x and 0x to 5x the MIC drug concentration added. Of these, only five lipids were seen to increase in concentration across from 0x to 1x to 5x ($[M+H]^+$): hydroxyphthioceranic acid (C33), DG (39:2), PE(34:1), PG(34:2) and PG(34:1). The same trends were seen in both **24** and **21** when tested against two separate control samples each (no drug added to culture). No trends were seen in **11**, as the data range was not extended far enough. Data for $[M-H]^-$ was less reliable, as most lipids were seen to be increasing in concentration contrary to what was seen in $[M+H]^+$ and by TLC, and was therefore not analysed any further.

Having found some leads whilst searching through individual lipids, attention was turned to a broader analysis, looking at cumulative intensity across ranges of 5 m/z values. Immediately it was clear that the differences between 1x and 5x MIC are larger for **21** than **24**. This can be rationalised, as **21** must be hydroxylated prior to any interactions with lipid biosynthesis according to our hypothesis, whereas **24** is in its active form. Therefore, smaller differences will be expected in **24**, as a larger volume of drug will be present at 1x MIC compared to **21**, so should impact lipid biosynthesis at lower concentrations.

Moreover, upon inspecting **24** more closely, it could be seen that there were particular more prominent bands found at 590-594, 690-694, 730-734, 775-779 and 1395-1399 m/z (Figure 2.6). Given the format of the graph, a larger, positive band indicates a larger reduction in

intensity, so a reduction is being observed in the bands displayed. Using the same constraints as previously, the raw data in these ranges were input into Lipid Maps® again, but searching for all positive adducts (H, Na, K, NH_4). 18 hits were found with Δ/mass ≤ 5 ppm: 15 of these were glycerophospholipids and the remaining three were MPM(C32), hydroxyphthioceranic acid (C36) and DG(31:1). Interestingly, when comparing the five hits from the initial search to the 18 hits of this search, each lipid class found originally was seen again, though with opposing trends. Although not conclusive, this lays a foundation for future studies into the effect of vanoxerine on cell wall biosynthesis.

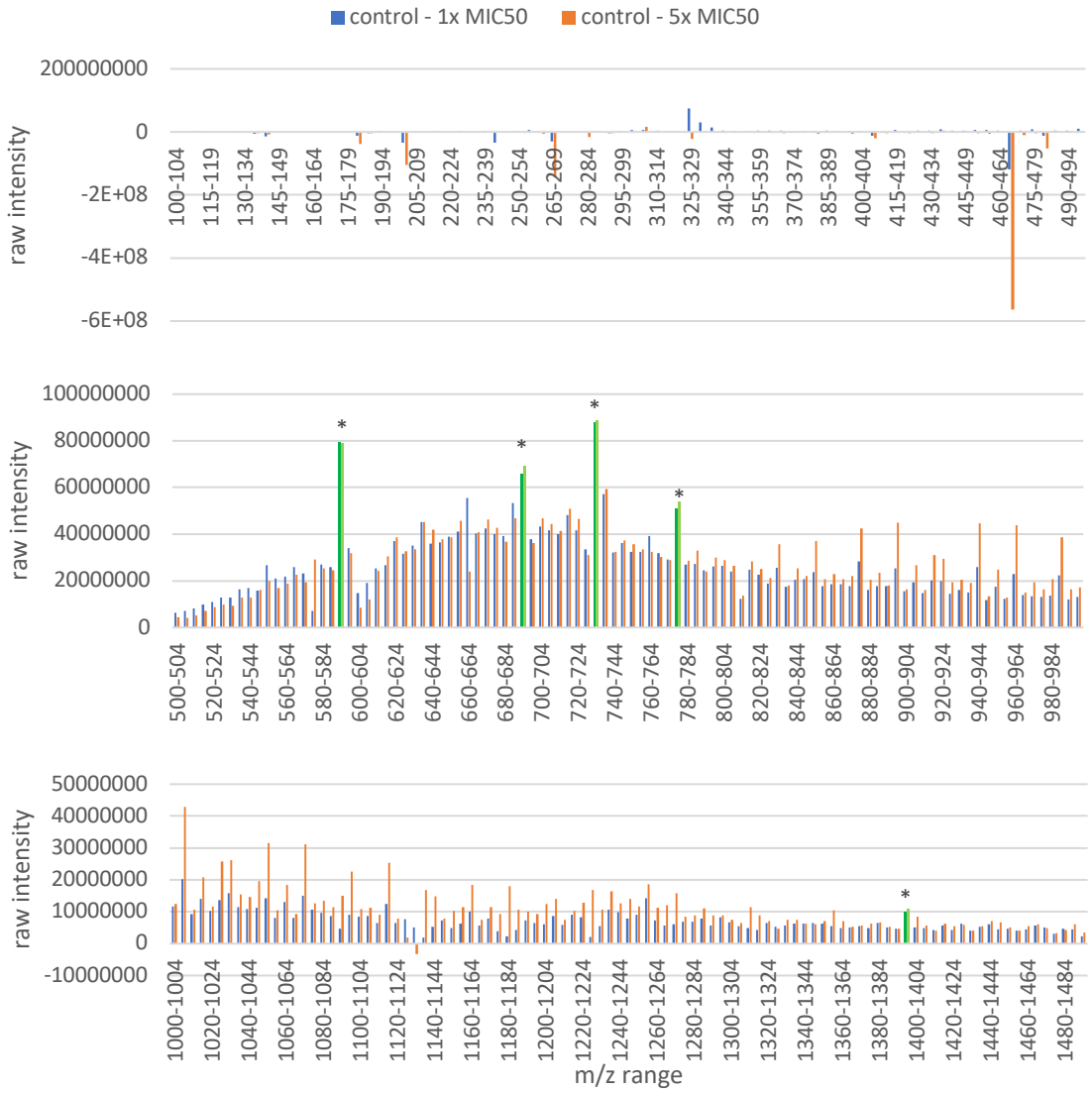


*Figure 0.6 Cumulative intensities of ESI+ mass spectrum readings for compound **24**, whereby m/z values were arranged into bins of 5 m/z difference. The values shown are the difference in raw intensity between a control (no drug added) and either the corresponding readings at 1x MIC value (blue) or 5x MIC value (orange) over a given range. Therefore, a positive bar highlights a bin where the intensity of a given compound or compounds has decreased when drug was added. A greater intensity is indicative of a greater reduction in the concentration of a given compound or compounds, suggesting a lipid biosynthetic pathway may have been altered. Five bins, highlighted green and marked with an asterisk, were studied further due to greater intensities than neighbouring bins.*

Subcloning of MSMEG_2240 and MSMEG_2038

As a further branch to the project, an attempt was made to subclone overexpressor genes of MSMEG_2038 and MSMEG_2240 into *E. coli* in order to express and purify the enzymes. The genes were previously incorporated into separate pVV16 vectors, which were each digested following transformation and amplification in *E. coli* T10 at the restriction sites HindIII and NdeI, liberating the gene. MSMEG_2240 was then ligated into a pET23b construct, yielding pET23b_2240, but incorporation of MSMEG_2038 was not achieved within the time constraints of the project. Each ligation was confirmed through a further double digest at the same restriction sites, yielding two bands after running on a 1% agarose gel (S1). Transformation of pET23b_2240 into *E. coli* T10 was then attempted, yielding a single colony across 10 plates. Amplification and isolation of the plasmid was followed by heat shock transformation into *E. coli* BL21(DE3) and *E. coli* T7 shuffle, which are both suitable strains for gene expression. Colonies were observed in both strains.

With regards to MSMEG_2038, although no heat shock transformations yielded *E. coli* T10 containing the desired plasmid, a control plate produced a single colony of *E. coli* T10 containing the empty pET23b vector. Therefore, although pET23b_2038 was not successfully constructed within the time constraints of this project, optimisation of the ligation and transformation conditions is likely to produce the desired plasmid.

Although time pressures prevented expression and purification of MSMEG_2240 in this project, future researchers will complete this to enable further structural and biochemical studies of the enzyme. Drug binding assays will be able to confirm or disprove the current hypothesis of hydroxylation of vanoxerine, hopefully in combination with crystal structures of MSMEG_2240 bound to vanoxerine.

Conclusion

Overall, significant advancements were made discovering vanoxerine's interactions in mycobacteria. Further evidence has been provided to support the theory of *in vivo* hydroxylation of vanoxerine by either MSMEG_2038 (Rv0565c), MSMEG_2240 (Rv3518c) or both, whilst preliminary results indicate that the drug may be acting upon cell wall biosynthesis pathways. Furthermore, with the successful cloning of MSMEG_2240 into *E. coli* BL21(DE3) and T7 shuffle, and the cloning of MSMEG_2038 close, isolation of the enzyme products will allow for more in depth studies of the interactions of enzymes with vanoxerine.

3. Tackling antimicrobial resistance in *Pseudomonas aeruginosa*: exploring 6-chloro-3-(thiazol-4-ylmethyl)quinazolin-4(*3H*)-one derivatives as antagonists of PqsR

Abstract

The Gram-negative bacterium *Pseudomonas aeruginosa* is a major opportunistic pathogen, which principally causes nosocomial infections and infections in cystic fibrosis patients. High levels of antibiotic resistance in this pathogen make it difficult to treat and reinfection is common. However, methods targeting virulence may attenuate the bacterium without affecting cell viability and hence treat infection without the risk of antibiotic resistant populations growing. This study expands on previous work targeting PqsR, an autoinductive transcription regulator in the *pqs* quorum sensing signalling system. A structure-activity relationship study yielded 16 compounds as potential PqsR antagonists. Of these, 11 compounds showed a degree of antagonism *via* a biosensor reporter assay, utilising a *P. aeruginosa* mCTX::P_{pqsA}-lux chromosomal promoter fusion in strains PA01-L and PA14. Further to this, IC_{50} assays are currently being undertaken for all compounds displaying some antagonism as shown by the biosensor reporter assay. At the time of writing testing has only been completed for compound **31g** showing an IC_{50} value of 1.26 μM. These results provide a starting point for an effective optimisation process in the search for drug-like PqsR antagonists.

Introduction

The antibiotic resistance crisis, though not a new phenomenon, is an ever-growing problem, which cannot be improved without novel approaches to challenging it. *P. aeruginosa* is an opportunistic Gram-negative bacterium, capable of causing acute and chronic infection. It is one of the leading causes of nosocomial infection, as well as one of the largest causes of death in cystic fibrosis sufferers due in part to its ability to form biofilms and its resistance to most antibiotics.[49-51] Reinfection is common and is generally caused by antibiotic resistant subpopulations which were present in the primary infection. As such, *P. aeruginosa* infection is a key example of a disease which will benefit substantially from novel approaches to the treatment of AMR. One hopeful route is the targeting of non-essential proteins, which can attenuate virulence without killing the non-resistant population; in doing so, it is predicted that

combination therapy with traditional antibiotics may treat infection in immunocompromised patients without relapse.[52-53]

One such area which has experienced increased levels of research is the targeting of quorum sensing pathways. Quorum sensing is the process by which bacteria utilise peptides and small organic molecules to modulate gene-expression across a population when threshold levels of autoinducers are met. In *P. aeruginosa* three distinct quorum sensing pathways exist: the *las* and *rhl* systems, which are both reliant on N-acyl-homoserine lactones (AHLs), and the *pqs* system, which is regulated by alkylquinolones (AQs).[54] These three systems intertwine[55] and have major effects across the population such as biofilm synthesis and the release of virulence factors.[5, 56] The *pqs* system has been shown to be involved in biofilm maturation and pyocyanin synthesis specifically through interactions between the natural agonists 2-heptyl-3-hydroxy-4(*1H*)-quinolone (PQS) and 2-heptyl-4-hydroxyquinolone (HHQ) with PqsR (Scheme 3.1), the transcriptional regulator which acts upon the *pqsABCDE* operon. Obstructing PqsR has been proven to reduce biofilm formation and the release of toxins, and therefore has been validated as a worthy target. As such, the development of PqsR antagonists is highly desirable in the search for novel antibiotics.

Previous research has led to the development of several distinct PqsR antagonists: structures were varied and have been based on quinazolinones,[56] benzamide-benzimidazoles,[57] amino-oxadiazoles[58] and quinolinones.[59] Lu *et al*. showed that converting the 3-position of quinolones to an amide,[59-60] such as that of HHQ-like **29**, turned potent agonists into potent antagonists, and since then research has led to the development of quinazolinones as anti-PqsR compounds (Figure 3.2). Subsequently, a virtual screening study (unpublished) elaborated on this structure, suggesting that thiazoles connected at the 3-position of a quinazolinone *via* a methyl linker could prove to be potent antagonists of PqsR.

Virtual screening is one of the most employed methods of identifying hit compounds. Its key benefit is that it enables a high volume of structures with varying functionalities to be tested *in silico* over a short amount of time, thus saving both time and money. Through structure-based virtual screening, compounds are designed around a known protein target in an attempt to identify potential bioactive molecules and scored based on how well they fit the protein model. Virtual screening can never give a definitive hit compound due to the multitude of variables and unpredictability when compounds are tested in biological assays, but through proper

implementation can provide a more informed basis for developing hit compounds than could be obtained by a researcher's own intuition alone.[61]

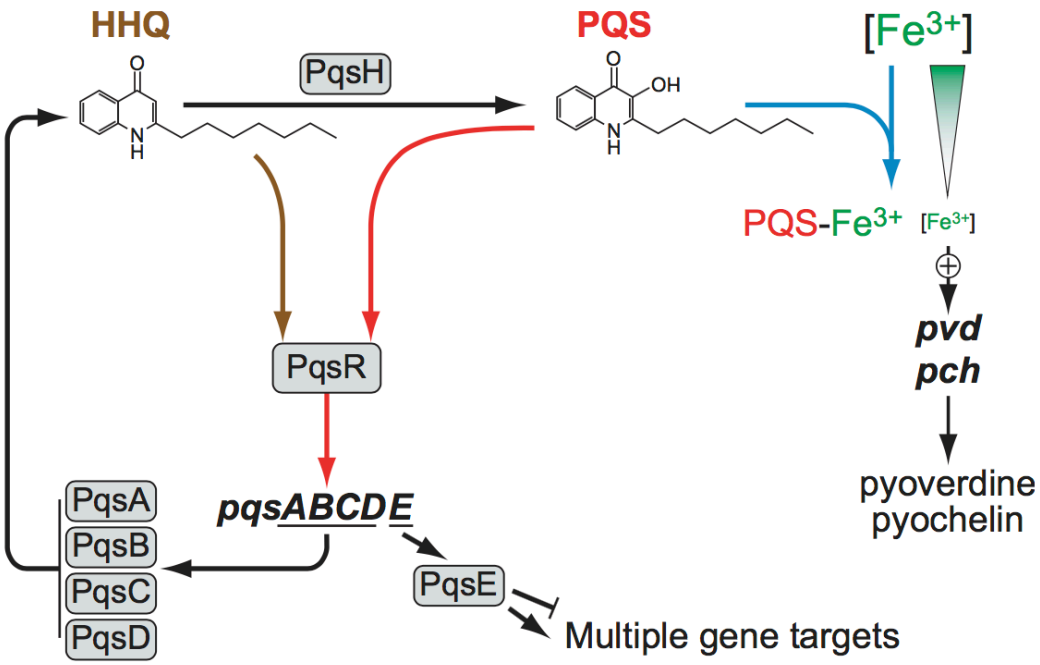
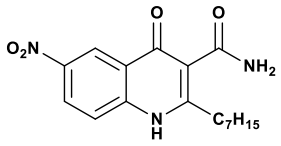
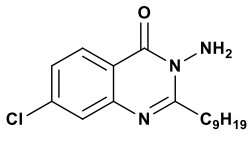


Figure 0.1 A simplified representation of the P. aeruginosa quorum sensing system (pqs). The autoinductive regulator, PqsR, can bind to two endogenous alkyl-quinolone (AQ) ligands, HHQ and PQS. Ligand binding promotes expression of pqsABCD which generate the production of further AQs. PQS has a greater agonistic effect than HHQ, which can be converted into the former through an enzyme controlled hydroxylation (PqsH). PQS has also been shown to display iron chelating effects and is a precursor to important virulence factors such as the siderophores pyoverdine and pyochelin. [Taken from Ilangovan et al. 2013].[5]

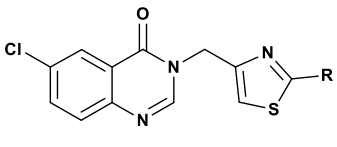
Continuing on from the aforementioned virtual screening study, this work looks to develop a range of substituted 3-(thiazol-4-ylmethyl)-4-quinazolin-4(*3H*)-one compounds to explore the effect of functionalisation at the 2-position of the thiazole ring based around the outputted data. It is believed that the space surrounding the 2-position is a hydrophobic pocket and as such a comprehensive SAR study was designed to explore this pocket and the ideal moiety that may fill it to improve affinity.



29.



30.



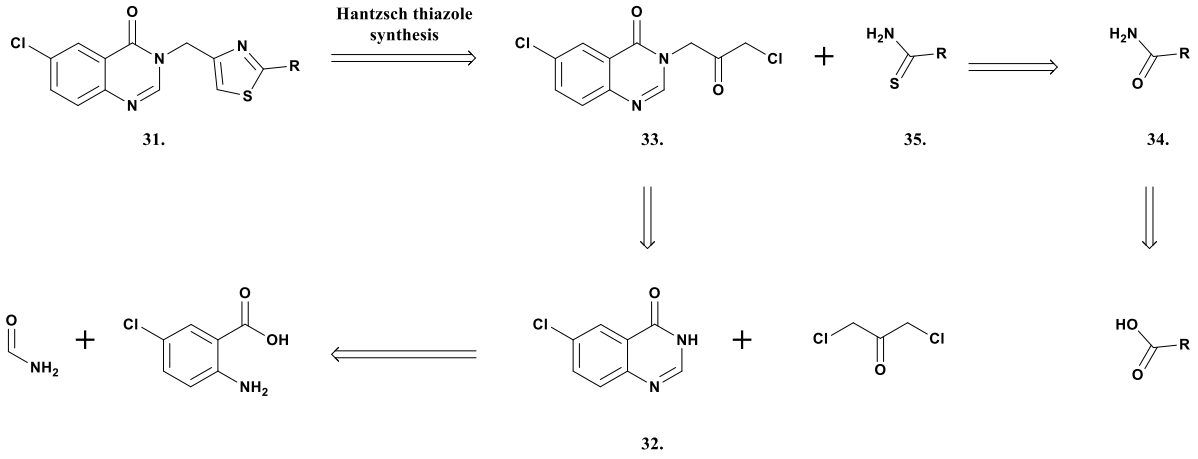
31.

*Figure 0.2 Previously published antagonists of PqsR include the amide functionalised quinolone **29** and the quinazolinone **30**. Quinolone **29** was based around the structure of HHQ, but the addition of amide and nitro moieties turned it from a potent agonist to a potent antagonist. It was further found that the addition of a nitrogen atom, turning it from a quinolone to a quinazolinone (**30**) boosted antagonism further. Compound **31** was developed through virtual screening and was chosen for further studies due to its core quinazolinone structure, which shares common features to the endogenous agonistic ligands HHQ and PQS.*

Results and Discussion

Synthesis of the quinazolinone precursor

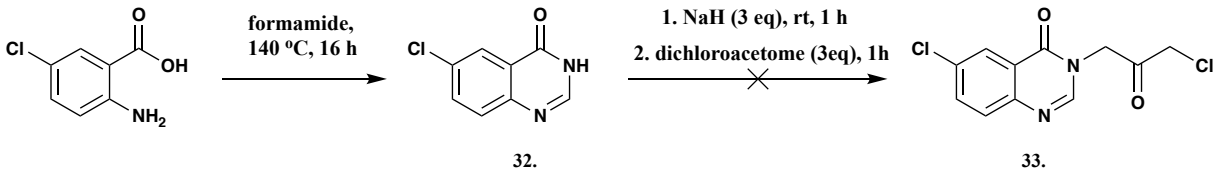
The formation of each analogue was deemed possible through one conserved reaction scheme, with the key reaction being a Hantzsch thiazole synthesis between an α-haloketone and varying thioamides. Initially, attempts were made to synthesise the α-haloketone in two steps: firstly 2-amino-5-chlorobenzoic acid was reacted with formamide, forming 6-chloroquinazolin-4(*3H*)-one in excellent yield. Subsequent attempts to alkylate the amine using 1,3-dichloroacetone were unsuccessful (Scheme 3.1).



*Scheme 0.1 The proposed retrosynthesis of the series of thiazoles **31** hinged around the Hantzsch thiazole synthesis, reacting an α-haloketone with a thioamide. The α-haloketone could be synthesised in a two-step procedure from 2-amino-5-chlorobenzoic acid, whilst the thioamides could be synthesised from carboxylic acids in two steps.*

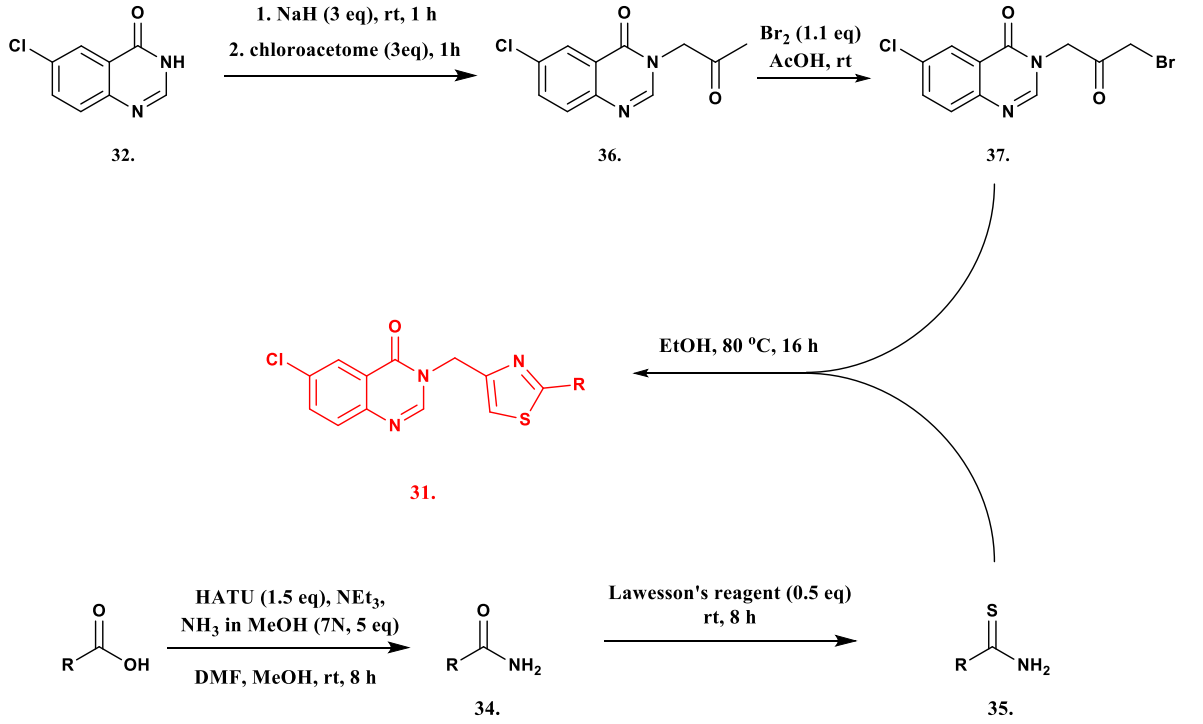
All attempted reactions focussed around deprotonation of the amine of **32** with a base, followed by addition of 1,3-dichloroacetone. Neither K_2CO_3 nor Cs_2CO_3 were found to yield any reaction regardless of solvent, temperature or duration of reaction. However, deprotonation with NaH in NMP, followed by a slow addition of 1,3-dichloroacetone led to the formation of a trace amount of product **33**. This could not be purified though, and a major unknown by-product formed in the process (Scheme 3.2). Therefore, an alternate approach was taken: as with scheme 3.1, the precursor **37** could simply be reacted with a thioamide to give the desired thiazole, but the route to **37** would be undertaken in a 3-step process. As seen in previous attempts, no reaction would occur between 6-chloroquinazolin-4(*3H*)-one and K_2CO_3 or Cs_2CO_3, but deprotonation with NaH and electrophilic attack with chloroacetone yielded the

acylated product in very good yield. Once again, NMP was the only suitable solvent, with others such as DMF, THF and acetonitrile failing to yield any product (Scheme 3.3).



32. 33.

Scheme 0.2 Synthesis of the intermediate 6-chloroquinazolinone was successful, but further alkylation with dichloroacetone was not possible. Trace amounts of product were observed after deprotonation with NaH in NMP, but the addition of dichloroacetone did not yield the desired product in large enough quantities and the trace amounts could not be purified.



32. 36. 37. 31. 34. 35.

*Scheme 0.3 A revised synthesis of **31** saw the α-haloketone formed over two steps from **32**. Alkylation with the same conditions which yielded trace amounts of the α-chloroketone (Scheme 3.2) yielded the 2-oxopropyl quinazolinone **36** in excellent yield. Whilst optimisation of the subsequent bromination step was required, good yields were obtained for **37** when dissolved in acetic acid with a dropwise addition of bromine. Thioamides were synthesised via the amidation of carboxylic acids in the presence of HATU and ammonia, following which stirring with Lawessons's reagent converted the amide into a thioamide.*

Various reaction conditions were trialled to then brominate the α-carbon of the ketone, but with minimal success initially. Reacting with *N*-bromosuccinimide (NBS) failed to yield any brominated species, although addition of a small volume of silica gel to acidify the mixture generated trace amounts of the desired monobrominated product. A small-scale reaction between **36** and trimethylphenylammonium tribromide yielded the desired product with 91% conversion as indicated by ^{1}H NMR, but could not be isolated. Upon scaling up this reaction failed to yield the same results, with conversion of 10% instead and the product could not be purified. The most successful bromination was achieved by dissolving **36** in acetic acid and reacting with bromine through a dropwise addition. Although a small amount of dibrominated

species was observed, the reaction went to completion and a yield of 66% was achieved without difficulty in the purification as had previously been observed.

Selection and synthesis of the thioamides

The initial aim of the project was to explore the region believed to be a hydrophobic pocket in PqsR, where the R-group of thiazole **31**, may sit. As such, the compounds designed varied only in the length and branching of an alkyl chain. Given that previous work has shown a nonyl chain at position C-2 to produce a potent antagonist, with some other substitutions, and that the natural agonist PQS has a heptyl chain at C-2 it was hypothesised that an alkyl chain at the 3-position may also fill the same space.

Further to analysing the ideal alkyl chain, studies were initiated looking into the effects of introducing heteroatoms and conjugated systems (Figure 3.3). All thioamides could be simply derived from their corresponding carboxylic acid or acid chlorides through a two-step process. The carboxylic acids were converted to primary amides through stirring with ammonia and HATU, following which stirring with Lawesson's reagent generated the desired thioamides. Yields over two steps were found to vary between 14-80%, but reactions proceeded cleanly with no by-products except those expected to form from HATU and Lawesson's reagent.

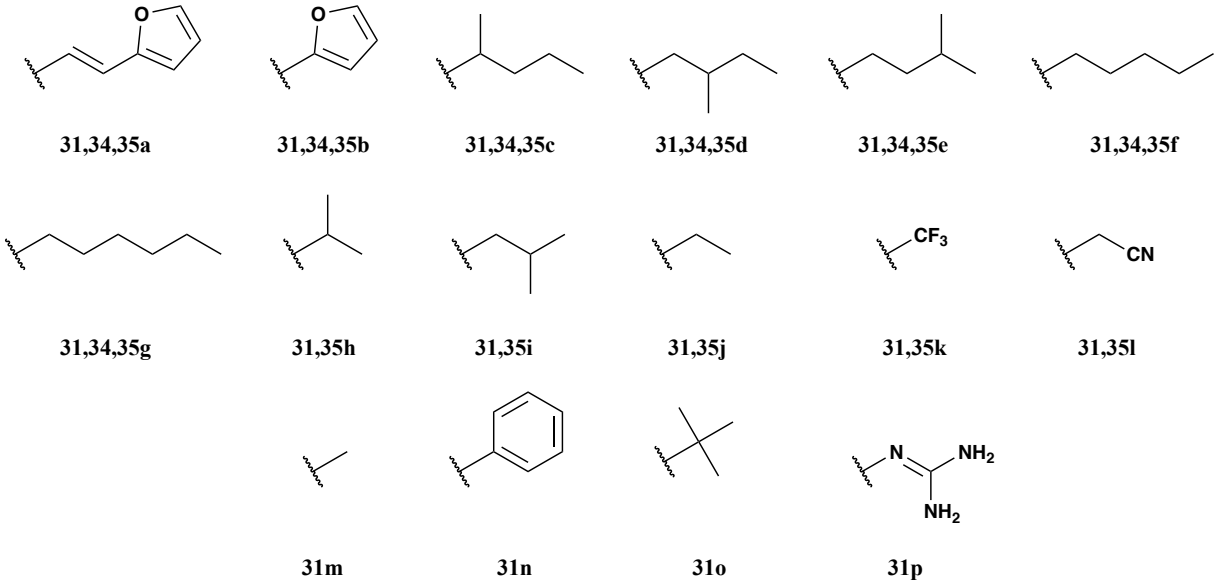
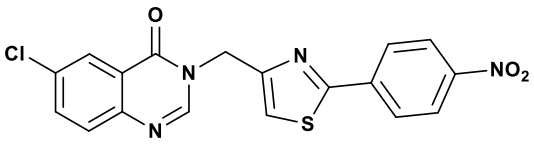
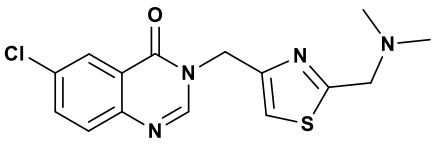


*Figure 0.3 The R-groups of successfully synthesised thiazoles. Compounds **a-g** used carboxylic acids as starting materials, which were amidated and converted to thioamides (**34** and **35** respectively), whilst compounds **i-l** were synthesised by directly converting amides to thioamides (**35**). Compounds **31m-31p** were synthesised by reacting α-bromoketone **37** with commercially available thioamides.*

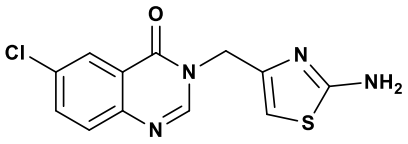
For the majority of compounds, thiazole formation was achieved through simple refluxing of precursor **37** and thioamide in ethanol without formation of by-products. However, for a select few compounds the thiazole did not form and unexpected results were seen. In the case of compounds **38** and **39** the precursor, under identical conditions to each other analogous reaction, was converted back to **36** with no other identifiable products in the reaction mixture. Furthermore, reaction of **37** with thiourea yielded no product and the only product identifiable by TLC was the thiourea itself (Figure 3.4). Aside from these limited cases though, Hantzsch thiazole syntheses yielded the desired product with yields between 12-91% and a wide range of analogues were synthesised, allowing for a comprehensive SAR study to be undertaken.



38.



39.



40.

*Figure 0.4 The structures of thiazoles which were not successfully synthesised. Compounds **38** and **39** showed evidence of degradation of the starting material, whereas compound **40** simply showed no reaction progression. Further optimisation of the Hanztsch thiazole synthesis is required, which may simply be a higher reaction temperature in the case of **40** or lower in the case of **38** and **39** to prevent degradation products forming.*

Biological testing

To efficiently test each compound's activity, a spot test was done, whereby a 10 μM sample was incubated in a PAO1-L mCTX::P_{pqsA}-lux strain. This mutant contains the *pqsA* gene fused to a bioluminescence marker, such that binding of an AQ to this sequence will generate luciferase LuxAB and generate light via bioluminescence.[62] Therefore, a reduction in bioluminescence is indicative of an antagonistic effect on PqsR. An identical test was also completed for each sample using PA14 mCTX::P_{pqsA}-lux, a similar but more virulent strain of *P. aeruginosa*. Within this assay, a remaining activity of 10% compared against the control is the baseline value which cannot be reduced further. As such, any compound shown to have a remaining activity around 10% is likely a potent antagonist. Similarly, compounds showing

activity between 20-50% are likely to be antagonists, but with a reduced affinity or efficacy (Figure 3.5).

Testing was completed for all synthesised compounds in both PA01-L and PA14. Given the increased virulence of PA14, testing usually shows the remaining activity to be slightly increased in PA14 compared to PA01-L. For the majority of compounds this was observed with the notable exceptions of **31g**,**l**,**n** and **p**. The reasons for these unexpected trends are not clear, though it could simply be a result of the simple nature of the assay; this assay is a semi-quantitative measure of whether a compound has antagonistic effects or not, and results are not definitive. Whilst it can clearly show whether a compound exhibits antagonism or not, further assays such as IC_{50} measurements are required to fully quantify each compound's effects, meaning the results from this assay have a small degree of ambiguity.

Five compounds were found to have a remaining activity below 20% in PA01-L, and a further five between 20-30%. In PA14 four were found to have a remaining activity below 20% and five were found between 20-30%. In general, those with low activities in PA01-L were also found to have low activities in PA14, but with some notable exceptions: **31c**,**d** and **e** all had low activities in PA01-L, but activity in PA14 was 10-15% higher for each compound. Although still showing antagonistic effects, these structures may be less suitable for further work than other structures given they share a common butyl chain core in the R-group. Conversely, structures **31g** and **o** show an increased antagonistic effect in PA14 over PA01-L. Regardless of slight variations between the tested strains, several key insights can be made into the structure-activity relationship of the tested compounds.

The initial aim of the SAR study was to determine the effects of different alkyl chains in the supposed hydrophobic pocket. To this end the results show clearly several key factors in determining efficacy: firstly, a longer alkyl chain improves efficacy in both strains. Compounds **31f** and **g** were two of the most potent compounds tested; **31f** was the second most potent compound tested on PA01-L and **31g** was the most potent against PA14. A general trend was seen, whereby shorter alkyl chains were less efficacious than longer chains. Compound **31i** was a mild antagonist, whereas **31c** and **e** were more potent, and **31f** and **g** were two of the most potent, as previously stated.

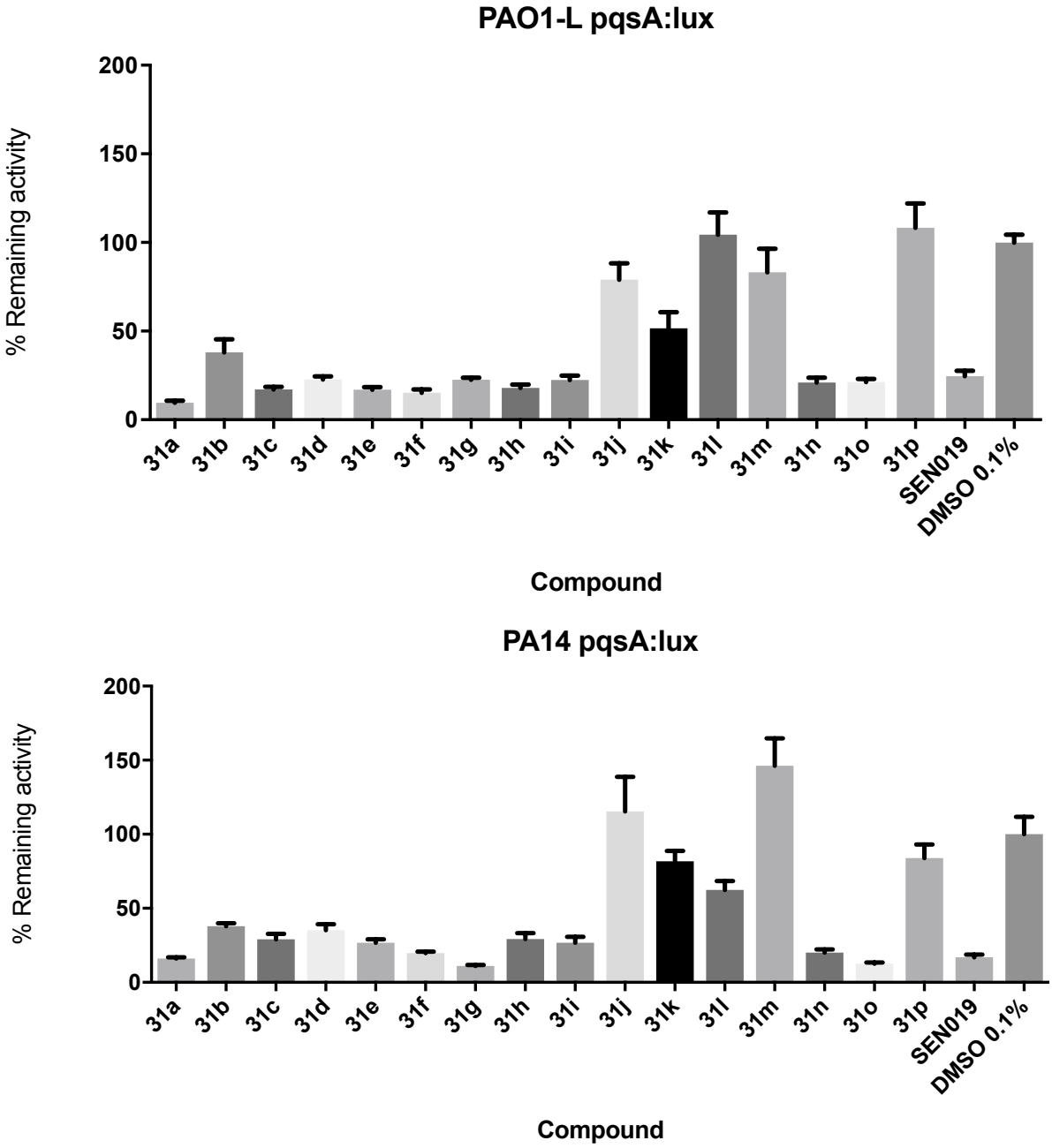


*Figure 0.5 Results of the biosensor reporter assay for all synthesised compounds in PA01-L (top) and PA14 (bottom). A pqsA::lux fusion strain of PA01-L and PA14 luminesces in the presence of AQs, which bind to PqsA and release LuxAB, a luciferase which causes bioluminescence. When an antagonist is introduced, PqsR is inhibited preventing the synthesis of HHQ and PQS, thereby reducing the luminescent activity. Controls of 0.1% DMSO (positive) and SEN019 (negative) were used, where SEN019 is a known antagonist developed in the Stocks group. A baseline activity of 10% is observed and hence activity of tested compounds will never drop below 10%. The results indicate that compounds with shorter alkyl chains (**31j-31m** were poor antagonists, whereas longer chains such as **31a**, **31f** and **31g** were more potent. Further quantitative analyses are required, such as IC_{50} assays for all compounds displaying antagonistic effects.*

Secondly, branching at the carbon neighbouring the thiazole appeared to vastly improve potency, as is shown by the low activity of **31h** in PA01-L; although the isopropyl group is far shorter than the other similarly potent compounds, it is far more potent than any other compound with either a similar molecular weight, or branching at a different carbon. Notably,

although a butyl chain is shown to be highly potent, compounds **31d** and **e**, with 3- and 4-methyl branched butyl chains respectively, are significantly less potent than **31c**. Moreover, compound **31o** with a *tert*-butyl group was the second most potent compound tested against PA14. This suggests a large vacancy directly adjacent to the thiazole ring, which could be exploited with further development of the compound series.

Another key trait shown by this data is that short alkyl chains have no effect on antagonism. Compounds **31j**,**k**,**m** and **l** each showed remaining activities above 50% in both PA01-L and PA14, evidence of a lack of antagonistic properties. Compounds **31j** and **m** showed remaining activity levels of 115% and 146% respectively in PA14, suggesting they may have agonistic properties as a result of the truncated alkyl chains. The final compound tested which had no antagonistic effect was **31p**, which is likely a result of a combination of two factors. Firstly, the compound was found to be extremely insoluble, having partially precipitated out in both DMSO and water. Therefore, assays may be affected by an apparent reduced concentration. Secondly, this compound is highly electronegative given the inclusion of three nitrogen atoms. Given that the presumed site of occupation is a hydrophobic pocket, there is likely to be strong repulsion and hence a poor affinity for this site.

The inclusion of heteroatoms and conjugated systems provided less obvious trends. As mentioned previously, compound **31p** had no antagonistic effects, possibly due to the fact that it contained three nitrogen atoms. However, the position of the heteroatoms may be an important factor; compound **31b** contained a furyl ring, which showed very weak antagonistic effects, whereas compound **31n** with a benzene ring showed much stronger antagonism. Given that both compounds have a similar size and planarity, they should occupy a similar region of PqsR's ligand binding domain. Therefore, any difference in activity is likely caused by the presence of the oxygen atom in **31b**, and hence the inclusion of the electronegative atom is causing a reduced affinity.

Moreover, compound **31a** contains a furyl group with an alkene linker and shows the strongest antagonism against PA01-L. Increasing the chain length increases activity, as is supported by the data from **31f** and **g**. The exact reason for its potency cannot be determined solely by this SAR study though. There are several key differences between **31a** and **31f** and **g**, namely the conjugation, the presence of a hydrogen bond acceptor and its planarity. Any of these could be the cause for its increased effects and further compound syntheses are needed to determine

each factor's contribution. Given the aforementioned conclusions on the effect of methyl groups at the 2-position, an interesting experiment would be mono- and geminal di-methylation of the alkene to observe how this alters antagonism.

One final noteworthy observation with regards to **31a** was that the submitted compound contained two isomers. Although it appeared to be clean by LC-MS, the NMR spectra showed the presence of a minor product. Whilst many peaks appeared to be shared from the quinazolinone and thiazole protons, there was a clearly separate alkene present. The minor product was seen at approximately 15% concentration of the major product but could not immediately be identified. Both major and minor products contained olefinic protons with *J*-coupling constants of approximately 16 Hz, suggesting both are *E*-alkenes. This leaves relatively few options of what the unknown isomer could be, but one likely candidate is that a 3-furyl bond has formed instead of a 2-furyl bond. The product was not a degradation product, as further NMR spectroscopy after storage at room temperature for one month showed an identical ^{1}H NMR spectrum. Although it is unlikely that the minor product is the cause of the potency, the compounds will be separated and tested individually to ensure the true activities are known.

Following on from the bioluminescence spot tests, IC_{50} testing was undertaken. At the time of writing, only compound **31g** has been tested, but all other compounds with antagonistic properties will follow. Tested only in PA01-L, **31g** was found to have an IC_{50} of 1.26 μM. Given that compound **31g** was found to be more potent against PA14 based on the bioluminescence assay, it is possible that this compound may have nanomolar efficacy against PA14, though only further assays will be able to prove this.

Conclusions

Within this project, a range of 6-chloro-3-(thiazol-4-ylmethyl)quinazolin-4(*3H*)-one derivatives were synthesized in an attempt to develop PqsR antagonists. Through a subsequent biosensor reporter assay, nine compounds were found to reduce PqsR activity significantly in both PA01-L and PA14, and will proceed to IC_{50} testing. Compound **31a** will be scrutinized in particular with respect to the effect of conjugation and further functionalization. Little has been confirmed as of yet with regards to the hydrophobic nature of the pocket examined, as most compounds featuring hydrogen bond donors and acceptors are either yet to be synthesized or tested. Therefore, further experimentation will determine whether polar groups are beneficial or a hindrance in this region. Overall though, a deeper insight was gained into optimisation of PqsR antagonists.

4. Future works and concluding remarks

The work accomplished for this thesis is just a snapshot of the overall effort needed for a project to succeed. As such, there is much work still to be completed continuing on from the groundwork laid here. The two projects detailed differ greatly in the process moving forward. With regards to the work associated with vanoxerine, here a compound with activity is known, but its mechanism of action is unclear. However, in the case of the PqsR project, a target is identified but the hit compound needs further development in order to make it more drug-like.

In the case of vanoxerine, it was hypothesised that vanoxerine is hydroxylated *in vivo* by either Rv3518c, Rv0565c or both. The process of *in vivo* hydroxylation has been proven with relative success, though the specific enzyme is yet to be deduced. Continuation of the subcloning work of MSMEG_2240 and MSMEG_2038 will enable overexpression and purification of the enzymes, which will allow for kinetic studies, such as isothermal titration calorimetry (ITC) to give binding affinities of vanoxerine to each enzyme. Furthermore, given the lack of understanding of the processes by which each of these enzymes functions, an explorative pull-down assay may be beneficial to understand any interactions they may have in the cell, for example with proteins associated with cell wall synthesis.

A more detailed understanding on vanoxerine's effects on lipid biosynthesis is pivotal to this study as this may give an insight into the effects vanoxerine may be having on cell wall biosynthesis. Although the TLC studies did indicate there was an accumulation of a lipid product as drug concentration was increased, this could not be identified and hence the specific pathway could not be elucidated. One simple method that could be employed to identify the compound would be to utilise preparative TLCs. Whilst direct analysis of the spot *via* TLC-MS yielded no results due to poor resolution, by preparing a preparative TLC as opposed to an analytical TLC the compound can be scratched off, purified and analysed by a mass spectrometer with greater resolution. This can then be compared against known libraries of mycobacterial lipids to identify its composition.

Although the intention of the project is to repurpose vanoxerine, the SAR study could be developed much further than has already been done. Given that it is being tested as an antimicrobial, as opposed to a CNS drug which was its initial identity, an optimisation process

may provide second generation drugs further down the pipeline. To date only the linker and one functionality has been altered for the SAR study. Changes to the two fluoro-phenyl groups may provide a more potent drug potentially, and currently work is being undertaken at the effects of removing one fluoro-phenyl group.

As stated previously, a select few compounds were highlighted which could not be synthesised. The immediate work following this will be to synthesise these, as well as several other derivatives of **31** in order to give a comprehensive SAR study. Moreover, a variety of functionalisations were highlighted which may be useful for understanding the true mechanisms of **31a**'s activity, which will also be explored. Further to this, 10 μM spot testing will be completed on the full set of compounds, as well as IC_{50} studies on the most potent selection within these.

However, this is not the only point at which the compound can be functionalised and following this project a study may be undertaken looking at optimisation of 3-thiazole-quinazolinones, in which additional positions may be functionalised or substituted. Should a lead compound come from this work it will be important to introduce solubilising groups without affecting the overall potency of the compound as a way of proving that there is scope to develop a drug-like molecule from it.

To further the PqsR project, an interesting development would be to obtain a crystal structure of the protein with a bound ligand. Previous attempts by others to purify the full protein have been unsuccessful, but the ligand binding domain has previously been successfully diffracted with antagonists co-crystallised. Therefore, co-crystallising one of the most successfully tested compounds would provide a useful insight into the binding of this series into the binding domain.

Should this be successful a second, more targeted SAR study could be undertaken, taking advantage of the images formed of the crystal structure. This would ideally focus on other moieties within the series which are yet to be explored, such as at the 2-position of the quinazolinone or the 5-position of the thiazole. Further optimisation may include attempts to add more solubilising groups in order to make the compound more drug-like. Currently, the

series has limited solubility in water, which would provide a major hurdle in the hit-to-lead optimisation process.

Finally, there have been various reported series of compounds which act as PqsR antagonists, but each has a distinct core from each of the others. The series detailed within this report was based upon the endogenous agonist PQS, but other potent compounds have no such basis. It may be possible to design hybrid compounds whereby the key elements of multiple series are incorporated into one designated scaffold. This effort will require a docking study and a comparison to all reported crystal structures of the ligand binding domain in order to assess the compatibility of different series with one another. However, should the different series adopt a similar conformation in the pocket, it is possible that a highly potent antagonist may be designed.

Each of the two projects detailed within approach the problem of antimicrobial resistance from a different perspective. There is no single solution to solving the crisis and it requires innovative thinking from all areas of science. Former prime minister David Cameron commissioned a review into tackling drug-resistant infection globally and in 2016 Jim O'Neill, the dedicated author, published his final recommendations on the subject. His warnings were stark, and should the rise in drug-resistant infections continue at its current rate, it is estimated that there will be a resultant 10 million deaths a year and a $100 trillion USD loss to the economy by 2050. It will only be through innovative solutions and multifaceted collaborations between the scientific community that this outcome can be avoided and stem the rise in antimicrobial resistance.

5. References

1. Wachino, J.; Yamaguchi, Y.; Mori, S.; Kurosaki, H.; Arakawa, Y.; Shibayama, K., Structural Insights into the Subclass B3 Metallo-β-Lactamase SMB-1 and the Mode of Inhibition by the Common Metallo-β-Lactamase Inhibitor Mercaptoacetate. *Antimicrob. Agents Chemother.* **2013,** *57*, 101-109.
2. Driscoll, M. D.; McLean, K. J.; Levy, C.; Mast, N.; Pikuleva, I. A.; Lafite, P.; Rigby, S. E. J.; Leys, D.; Munro, A. W., Structural and Biochemical Characterization of *Mycobacterium tuberculosis* CYP142: Evidence for Multiple Cholesterol 27-Hydroxylase Activities in a Human Pathogen. *J. Biol. Chem.* **2010,** *285*, 38270-38282.
3. Otero, L. H.; Rojas-Altuve, A.; Llarrull, L. I.; Carrasco-López, C.; Kumarasiri, M.; Lastochkin, E.; Fishovitz, J.; Dawley, M.; Hesek, D.; Lee, M.; Johnson, J. W.; Fisher, J. F.; Chang, M.; Mobashery, S.; Hermoso, J. A., How Allosteric Control of *Staphylococcus aureus* Penicillin Binding Protein 2a Enables Methicillin Resistance and Physiological Function. *Proc. Natl. Acad. Sci.* **2013,** *110*, 16808-16813.
4. Bansal-Mutalik, R.; Nikaido, H., Mycobacterial Outer Membrane is a Lipid Bilayer and the Inner Membrane is Unusually Rich in Diacyl Phosphatidylinositol Dimannosides. *Proc. Natl. Acad. Sci.* **2014,** *111*, 4958.
5. Ilangovan, A.; Fletcher, M.; Rampioni, G.; Pustelny, C.; Rumbaugh, K.; Heeb, S.; Cámara, M.; Truman, A.; Chhabra, S. R.; Emsley, J.; Williams, P., Structural Basis for Native Agonist and Synthetic Inhibitor Recognition by the *Pseudomonas aeruginosa* Quorum Sensing Regulator PqsR (MvfR). *PLoS Pathog.* **2013,** *9*, e1003508.
6. Fleming, A., On the Antibacterial Action of Cultures of a *Penicillium*, with Special Reference to their Use in the Isolation of *B. influenzæ*. *Br. J. Exp. Pathol.* **1929,** *10*, 226-236.
7. Giuliano, C.; Haase, K. K.; Hall, R., Use of Vancomycin Pharmacokinetic–Pharmacodynamic Properties in the Treatment of MRSA Infections. *Expert Rev. Anti-Infect. Ther.* **2010,** *8*, 95-106.
8. Grave, K.; Torren-Edo, J.; Mackay, D., Comparison of the Sales of Veterinary Antibacterial Agents Between 10 European Countries. *J. Antimicrob. Chemother.* **2010,** *65*, 2037-2040.
9. Dibner, J. J.; Richards, J. D., Antibiotic Growth Promoters in Agriculture: History and Mode of Action. *Poult. Sci.* **2005,** *84*, 634-643.
10. Batchelor, F. R.; Doyle, F. P.; Nayler, J. H. C.; Rolinson, G. N., Synthesis of Penicillin: 6-Aminopenicillanic Acid in Penicillin Fermentations. *Nature* **1959,** *183*, 257.
11. Oshiro, B. T., The Semisynthetic Penicillins. *Primary Care Update for OB/GYNS* **1999,** *6*, 56-60.
12. Schatz, A.; Bugie, E.; Waksman, S. A., Streptomycin, a Substance Exhibiting Antibiotic Activity Against Gram-Positive and Gram-Negative Bacteria. *Proc. Soc. Exp. Biol. Med.* **1944,** *55*, 66-69.
13. Geraci, J. E.; Heilman, F. R.; Nichols, D. R.; Wellman, W. E.; Ross, G. T., Some Laboratory and Clincical Experiences with a new Antibiotic, Vancomycin. *J. Lab. Clin. Med.* **1956,** *48*, 809-810.
14. Watt, L.; Jennison, R. F., Clinical Evaluation of Metronidazole- a new Systemic Trichomonacide. *Br. Med. J.* **1960,** *2*, 902-905.
15. Sauvage, E.; Kerff, F.; Terrak, M.; Ayala, J. A.; Charlier, P., The Penicillin-Binding Proteins: Structure and Role in Peptidoglycan Biosynthesis. *FEMS Microbiol. Rev.* **2008,** *32*, 234-258.
16. Vollmer, W.; Blanot, D.; De Pedro, M. A., Peptidoglycan Structure and Architecture. *FEMS Microbiol. Rev.* **2008,** *32*, 149-167.

17. Straus, S. K.; Hancock, R. E. W., Mode of Action of the New Antibiotic for Gram-Positive Pathogens Daptomycin: Comparison with Cationic Antimicrobial Peptides and Lipopeptides. *Biochim. Biophys. Acta, Biomembr.* **2006,** *1758*, 1215-1223.
18. Shinabarger, D. L.; Marotti, K. R.; Murray, R. W.; Lin, A. H.; Melchior, E. P.; Swaney, S. M.; Dunyak, D. S.; Demyan, W. F.; Buysse, J. M., Mechanism of Action of Oxazolidinones: Effects of Linezolid and Eperezolid on Translation Reactions. *Antimicrob. Agents Chemother.* **1997,** *41*, 2132-2136.
19. Hancock, R. E. W., Aminoglycoside Uptake and Mode of Action—with Special Reference to Streptomycin and Gentamicin. Antagonists and Mutants. *J. Antimicrob. Chemother.* **1981,** *8*, 249-276.
20. Bradford, P. A., Tigecycline: a First in Class Glycylcycline. *Clin. Microbiol. Newsl.* **2004,** *26*, 163-168.
21. Floss, H. G.; Yu, T.-W., Rifamycin: Mode of Action, Resistance, and Biosynthesis. *Chem. Rev.* **2005,** *105*, 621-632.
22. Smith, J. T., The Mode of Action of 4-Quinolones and Possible Mechanisms of Resistance. *J. Antimicrob. Chemother.* **1986,** *18* (Supplement_D), 21-29.
23. Fisher, J. F.; Meroueh, S. O.; Mobashery, S., Bacterial Resistance to β-Lactam Antibiotics: Compelling Opportunism, Compelling Opportunity. *Chem. Rev.* **2005,** *105*, 395-424.
24. Ghuysen, J. M., Serine Beta-Lactamases and Penicillin-Binding Proteins. *Annu. Rev. Microbiol.* **1991,** *45*, 37-67.
25. Bush, K.; Jacoby, G. A., Updated Functional Classification of β-Lactamases. *Antimicrob. Agents Chemother.* **2010,** *54*, 969-976.
26. Koike, T.; Takamura, M.; Kimura, E., Role of Zinc(II) in beta-Lactamase II: A Model Study with a Zinc(II)-Macrocyclic Tetraamine (1,4,7,10-Tetraazacyclododecane, Cyclen) Complex. *J. Am. Chem. Soc.* **1994,** *116*, 8443-8449.
27. Sulton, D.; Pagan-Rodriguez, D.; Zhou, X.; Liu, Y.; Hujer, A. M.; Bethel, C. R.; Helfand, M. S.; Thomson, J. M.; Anderson, V. E.; Buynak, J. D.; Ng, L. M.; Bonomo, R. A., Clavulanic Acid Inactivation of SHV-1 and the Inhibitor-resistant S130G SHV-1 β-Lactamase: Insights into the Mechanism of Inhibition. *J. Biol. Chem.* **2005,** *280*, 35528-35536.
28. Bush, K.; Macalintal, C.; Rasmussen, B. A.; Lee, V. J.; Yang, Y., Kinetic Interactions of Tazobactam with Beta-Lactamases from all Major Structural Classes. *Antimicrob. Agents Chemother.* **1993,** *37*, 851-858.
29. Hartman, B. J.; Tomasz, A., Low-Affinity Penicillin-Binding Protein Associated with Beta-Lactam Resistance in *Staphylococcus aureus*. *J. Bacteriol.* **1984,** *158*, 513-516.
30. Pucci, M. J.; Dougherty, T. J., Direct Quantitation of the Numbers of Individual Penicillin-Binding Proteins per Cell in *Staphylococcus aureus*. *J. Bacteriol.* **2002,** *184*, 588-591.
31. Sarkar, S. K.; Dutta, M.; Chowdhury, C.; Kumar, A.; Ghosh, A. S., PBP5, PBP6 and DacD Play Different Roles in Intrinsic β-Lactam Resistance of *Escherichia coli*. *Microbiol.* **2011,** *157*, 2702-2707.
32. Wagner, S.; Sommer, R.; Hinsberger, S.; Lu, C.; Hartmann, R. W.; Empting, M.; Titz, A., Novel Strategies for the Treatment of *Pseudomonas aeruginosa* Infections. *J. Med. Chem.* **2016,** *59*, 5929-5969.
33. World Health Organisation *Global Tuberculosis Report 2017*; Geneva: World Health Organisation, 2017.
34. European Centre for Disease Prevention and Control/WHO Regional Office for Europe *Tuberculosis Surveillance and Monitoring in Europe 2013*; Stockholm: European Centre for Disease Prevention and Control, 2013.

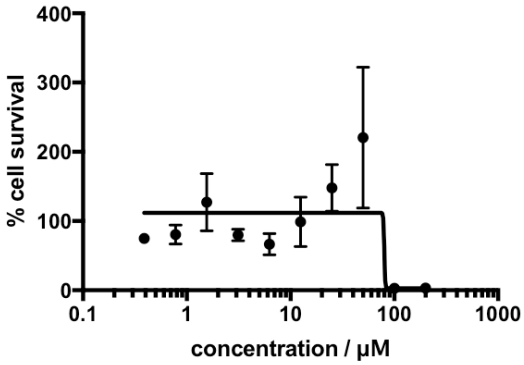
35. Bantubani, N.; Kabera, G.; Connolly, C.; Rustomjee, R.; Reddy, T.; Cohen, T.; Pym, A. S., High Rates of Potentially Infectious Tuberculosis and Multidrug-Resistant Tuberculosis (MDR-TB) among Hospital Inpatients in KwaZulu Natal, South Africa Indicate Risk of Nosocomial Transmission. *PLoS One* **2014,** *9*, e90868.
36. Oprea, T. I.; Mestres, J., Drug Repurposing: Far Beyond New Targets for Old Drugs. *AAPS J.* **2012,** *14*, 759-763.
37. Novac, N., Challenges and Opportunities of Drug Repositioning. *Trends Pharmacol. Sci.* **2013,** *34*, 267-272.
38. Palomino, J. C.; Martin, A., Is Repositioning of Drugs a Viable Alternative in the Treatment of Tuberculosis? *J. Antimicrob. Chemother.* **2013,** *68*, 275-283.
39. Alderwick, L. J.; Harrison, J.; Lloyd, G. S.; Birch, H. L., The Mycobacterial Cell Wall—Peptidoglycan and Arabinogalactan. *Cold Spring Harbor Perspect. Med.* **2015,** *5*, a021113.
40. Jankute, M.; Cox, J. A. G.; Harrison, J.; Besra, G. S., Assembly of the Mycobacterial Cell Wall. *Annu. Rev. Microbiol.* **2015,** *69*, 405-423.
41. Preti, A., Vanoxerine National Institute on Drug Abuse. *Curr. Opin. Invest. Drugs* **2000,** *1*, 241-251.
42. Herman, B. H.; Elkashef, A.; Vocci, F., Medications for the Treatment of Cocaine Addiction: Emerging Candidates. *Drug Discov Today: Ther. Strategies* **2005,** *2*, 87-92.
43. Hu, Y.; Van Der Geize, R.; Besra, G. S.; Gurcha, S. S.; Liu, A.; Rohde, M.; Singh, M.; Coates, A., 3-Ketosteroid 9α-Hydroxylase is an Essential Factor in the Pathogenesis of *Mycobacterium tuberculosis*. *Mol. Microbiol.* **2010,** *75*, 107-121.
44. He, Z.; De Buck, J., Cell Wall Proteome Analysis of *Mycobacterium smegmatis* Strain MC^2 155. *BMC Microbiol.* **2010,** *10*, 121.
45. Mahairas, G. G.; Sabo, P. J.; Hickey, M. J.; Singh, D. C.; Stover, C. K., Molecular Analysis of Genetic Differences Between *Mycobacterium bovis* BCG and Virulent *M. bovis*. *J. Bacteriol.* **1996,** *178*, 1274-82.
46. O'Sullivan, L. M.; Patel, S.; Ward, J. M.; Woodley, J. M.; Doig, S. D., Large Scale Production of Cyclohexanone Monooxygenase from *Escherichia coli* TOP10 pQR239. *Enzyme Microb. Technol.* **2001,** *28*, 265-274.
47. Jeong, H.; Barbe, V.; Lee, C. H.; Vallenet, D.; Yu, D. S.; Choi, S.-H.; Couloux, A.; Lee, S.-W.; Yoon, S. H.; Cattolico, L.; Hur, C.-G.; Park, H.-S.; Ségurens, B.; Kim, S. C.; Oh, T. K.; Lenski, R. E.; Studier, F. W.; Daegelen, P.; Kim, J. F., Genome Sequences of *Escherichia coli* B strains REL606 and BL21(DE3). *J. Mol. Biol.* **2009,** *394*, 644-652.
48. Lobstein, J.; Emrich, C. A.; Jeans, C.; Faulkner, M.; Riggs, P.; Berkmen, M., Shuffle, a Novel *Escherichia coli* Protein Expression Strain Capable of Correctly Folding Disulfide Bonded Proteins in its Cytoplasm. *Microb. Cell Fact.* **2012,** *11*, 753.
49. Micek, S. T.; Wunderink, R. G.; Kollef, M. H.; Chen, C.; Rello, J.; Chastre, J.; Antonelli, M.; Welte, T.; Clair, B.; Ostermann, H.; Calbo, E.; Torres, A.; Menichetti, F.; Schramm, G. E.; Menon, V., An International Multicenter Retrospective Study of *Pseudomonas aeruginosa* Nosocomial Pneumonia: Impact of Multidrug Resistance. *Crit. Care* **2015,** *19*, 219.
50. Price, K. E.; Naimie, A. A.; Griffin, E. F.; Bay, C.; O'Toole, G. A., Tobramycin-Treated *Pseudomonas aeruginosa* PA14 Enhances *Streptococcus constellatus* 7155 Biofilm Formation in a Cystic Fibrosis Model System. *J. Bacteriol.* **2016,** *198*, 237-247.
51. Winstanley, C.; O'Brien, S.; Brockhurst, M. A., *Pseudomonas aeruginosa* Evolutionary Adaptation and Diversification in Cystic Fibrosis Chronic Lung Infections. *Trend Microbiol.* **2016,** *24*, 327-337.
52. Christensen, L. D.; van Gennip, M.; Jakobsen, T. H.; Alhede, M.; Hougen, H. P.; Høiby, N.; Bjarnsholt, T.; Givskov, M., Synergistic Antibacterial Efficacy of Early Combination

Treatment with Tobramycin and Quorum-Sensing Inhibitors Against *Pseudomonas aeruginosa* in an Intraperitoneal Foreign-Body Infection Mouse Model. *J. Antimicrob. Chemother.* **2012,** *67*, 1198-1206.
53. Hentzer, M.; Wu, H.; Andersen, J. B.; Riedel, K.; Rasmussen, T. B.; Bagge, N.; Kumar, N.; Schembri, M. A.; Song, Z.; Kristoffersen, P.; Manefield, M.; Costerton, J. W.; Molin, S.; Eberl, L.; Steinberg, P.; Kjelleberg, S.; Høiby, N.; Givskov, M., Attenuation of *Pseudomonas aeruginosa* Virulence by Quorum Sensing Inhibitors. *EMBO J.* **2003,** *22*, 3803-3815.
54. Wilder, C. N.; Diggle, S. P.; Schuster, M., Cooperation and Cheating in *Pseudomonas aeruginosa*: the Roles of the *las, rhl* and *pqs* Quorum-Sensing Systems. *ISME J.* **2011,** *5*, 1332.
55. McGrath, S.; Wade, D. S.; Pesci, E. C., Dueling Quorum Sensing Systems in *Pseudomonas aeruginosa* Control the Production of the Pseudomonas Quinolone Signal (PQS). *FEMS Microbiol. Lett.* **2004,** *230*, 27-34.
56. Soukarieh, F.; Vico Oton, E.; Dubern, J. F.; Gomes, J.; Halliday, N.; de Pilar Crespo, M.; Ramirez-Prada, J.; Insuasty, B.; Abonia, R.; Quiroga, J.; Heeb, S.; Williams, P.; Stocks, M. J.; Camara, M., *In Silico* and *in Vitro*-Guided Identification of Inhibitors of Alkylquinolone-Dependent Quorum Sensing in *Pseudomonas aeruginosa*. *Molecules* **2018,** *23* 257 doi:10.3390/molecules23020257.
57. Starkey, M.; Lepine, F.; Maura, D.; Bandyopadhaya, A.; Lesic, B.; He, J.; Kitao, T.; Righi, V.; Milot, S.; Tzika, A.; Rahme, L., Identification of Anti-virulence Compounds That Disrupt Quorum-Sensing Regulated Acute and Persistent Pathogenicity. *PLoS Pathog.* **2014,** *10*, e1004321.
58. Zender, M.; Klein, T.; Henn, C.; Kirsch, B.; Maurer, C. K.; Kail, D.; Ritter, C.; Dolezal, O.; Steinbach, A.; Hartmann, R. W., Discovery and Biophysical Characterization of 2-Amino-oxadiazoles as Novel Antagonists of PqsR, an Important Regulator of *Pseudomonas aeruginosa* Virulence. *J. Med. Chem.* **2013,** *56*, 6761-6774.
59. Cenbin, L.; K., M. C.; Benjamin, K.; Anke, S.; W., H. R., Overcoming the Unexpected Functional Inversion of a PqsR Antagonist in *Pseudomonas aeruginosa*: An *In Vivo* Potent Antivirulence Agent Targeting *pqs* Quorum Sensing. *Angew. Chem. Int. Edit.* **2014,** *53*, 1109-1112.
60. Shanahan, R.; Reen, F. J.; Cano, R.; O'Gara, F.; McGlacken, G. P., The Requirements at the C-3 Position of Alkylquinolones for Signalling in *Pseudomonas aeruginosa*. *Org. Biomol. Chem.* **2017,** *15*, 306-310.
61. Scior, T.; Bender, A.; Tresadern, G.; Medina-Franco, J. L.; Martínez-Mayorga, K.; Langer, T.; Cuanalo-Contreras, K.; Agrafiotis, D. K., Recognizing Pitfalls in Virtual Screening: A Critical Review. *J. Chem. Inf. Model.* **2012,** *52*, 867-881.
62. Fletcher, M. P.; Diggle, S. P.; Cámara, M.; Williams, P., Biosensor-Based Assays for PQS, HHQ and Related 2-Alkyl-4-Quinolone Quorum Sensing Signal Molecules. *Nat. Protoc.* **2007,** *2*, 1254.

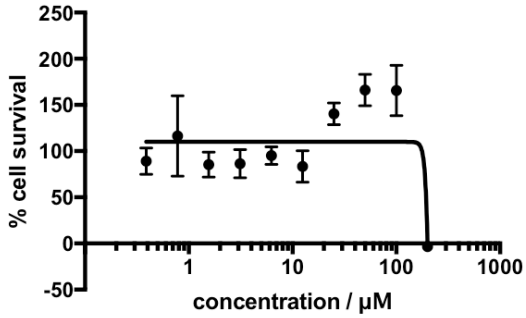
S1- Additional data for chapter 2

MIC_{50} Assays *M. Bovis* BCG

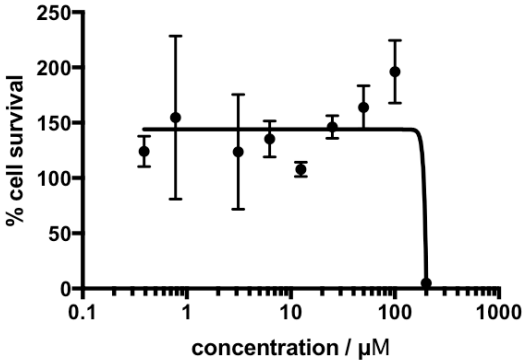
11



21

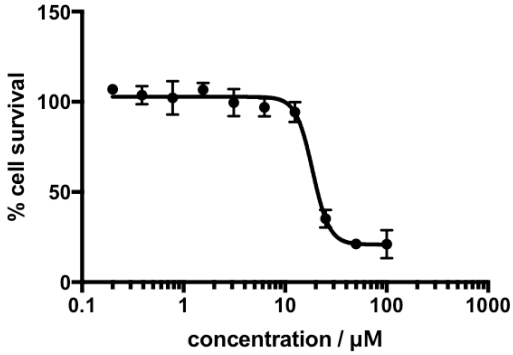


24

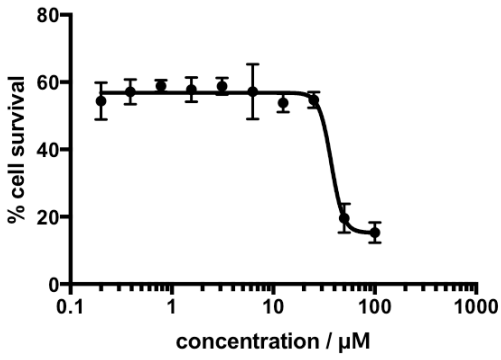


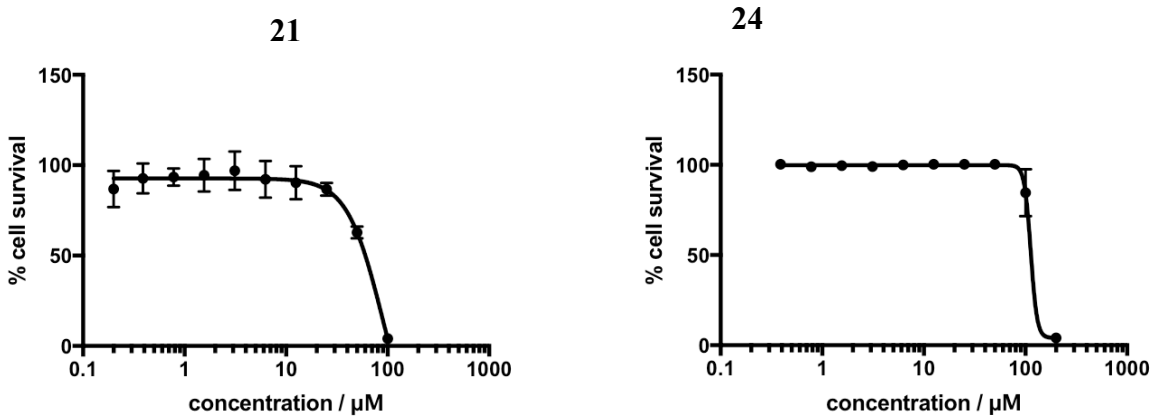
MIC_{50} Assays Vanoxerine Resistant *M. smegmatis* Mutants

11

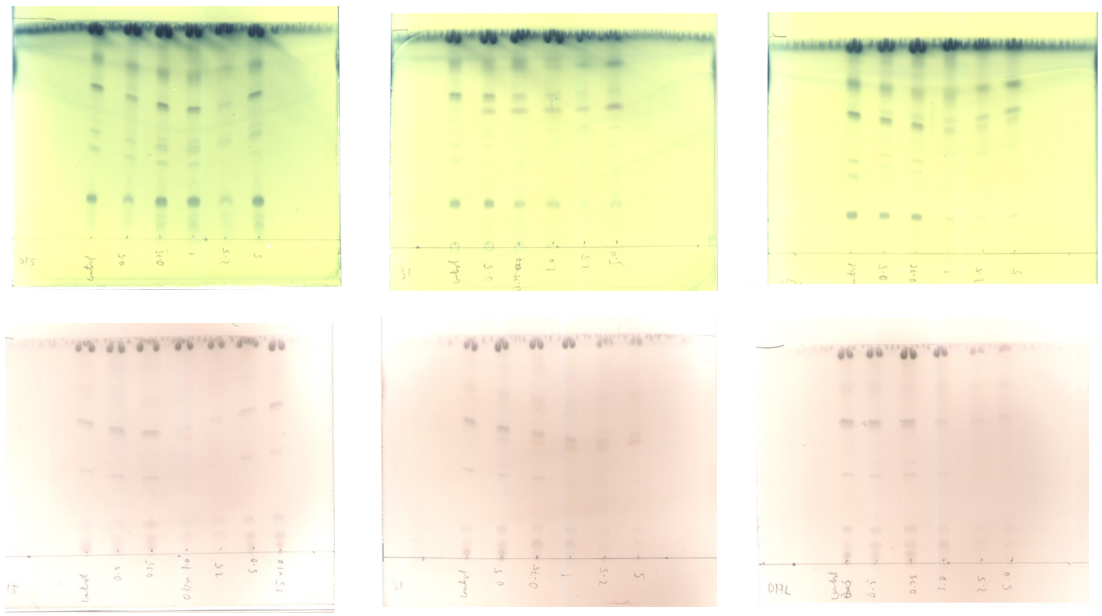


17

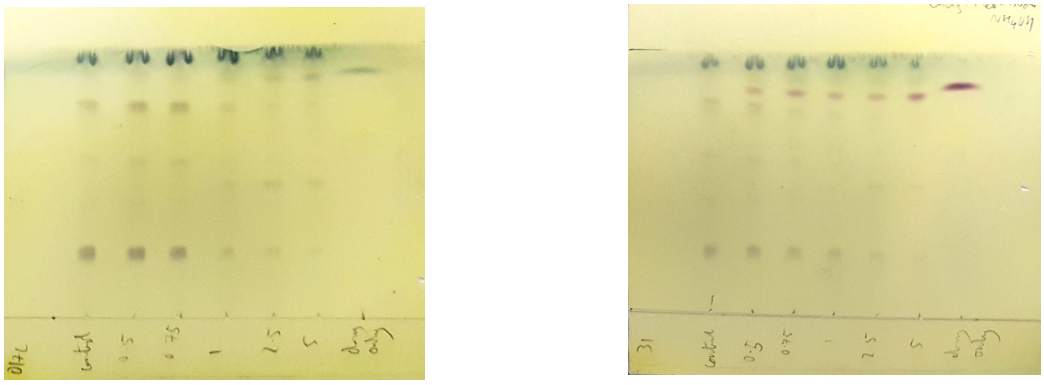




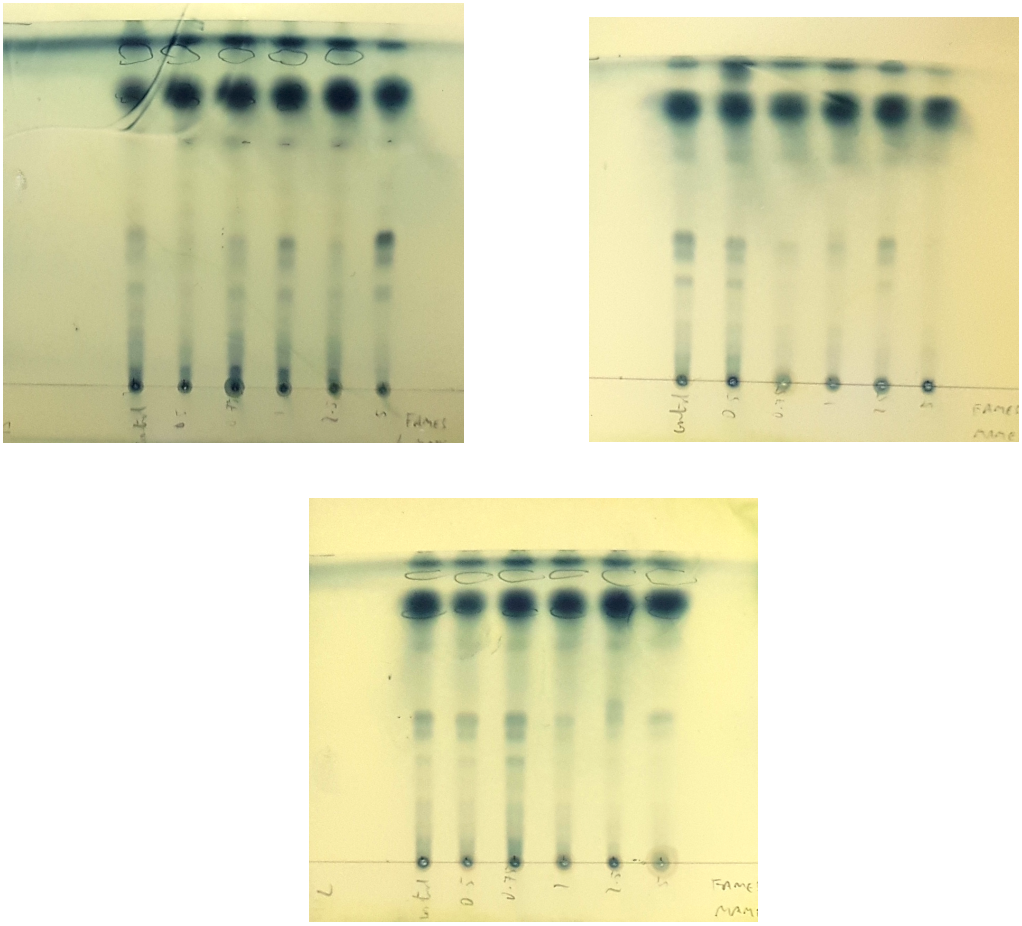
TLCs in Alternate Solvent Systems



*$CHCl_3$/MeOH/dH_2O 60:16:2 stained in polymolybdic acid (top) and α-naphthol (bottom): (left to right) compound **11**, **21** and **24***

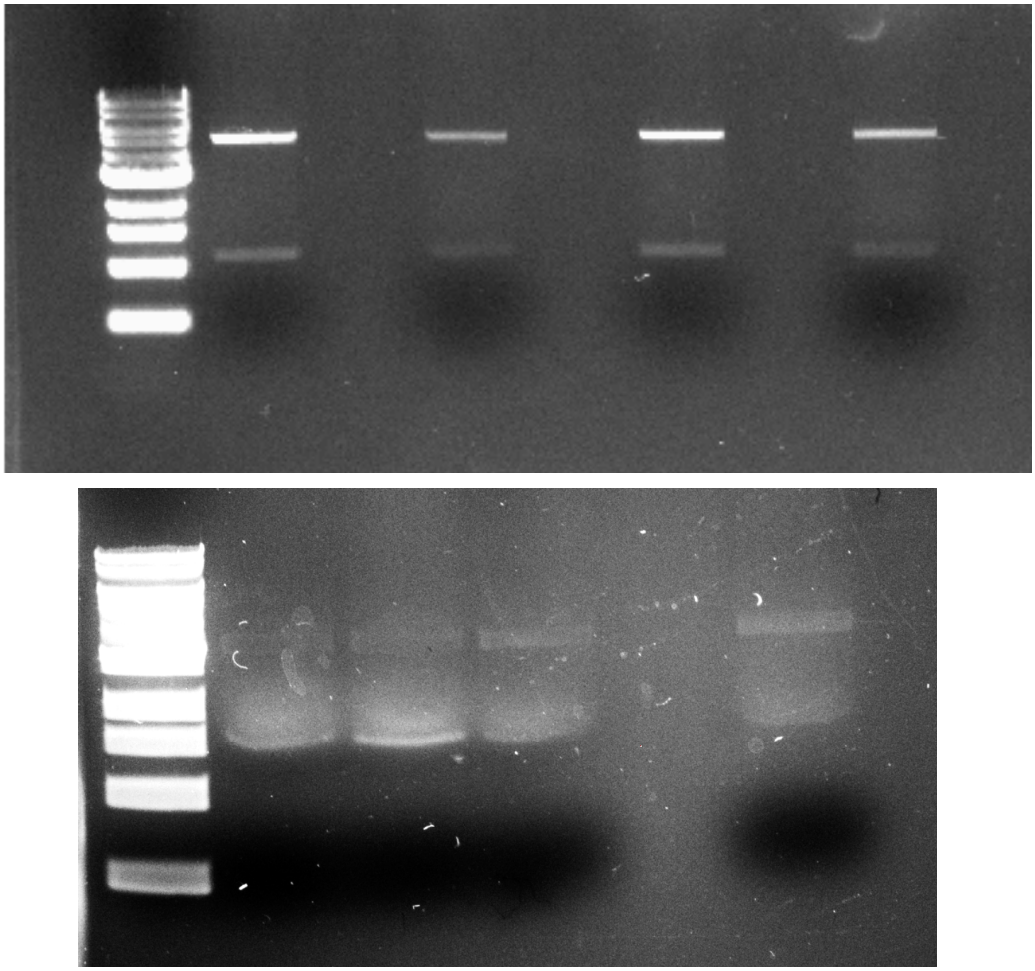


$CHCl_3$/MeOH/NH_4OH (80:20:2): (left) ***24*** *and (right)* ***21***



FAMEs and MAMEs extraction: (top left clockwise) ***11***, ***21*** *and* ***24***

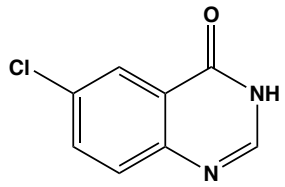
Plasmid Double Digest Gels



(top) double digest of pVV16_2240, and (bottom) double digest of pET23b_2240

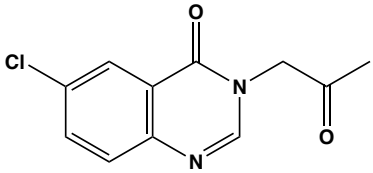
S2 – Experimental procedures for chapter 3

6-chloroquinazolin-4(3H)-one (32):



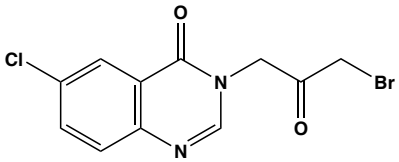
A solution of 2-amino-5-chlorobenzoic acid (4.99 g, 29.00 mmol) and formamide (20 mL) was refluxed at 140 ºC for 16 h during which time a brown precipitate formed. After cooling to room temperature, ice was added to aid in precipitation and the precipitate filtered and dried in vacuo, yielding **32** (5.13 g, 97%) as a brown solid: R_f = 0.29 (19:1, DCM/MeOH); ^{1}H NMR (DMSO-d_6, 400 MHz) δ 12.44 (br s, 1H), 8.12 (s, 1H), 8.06 (d, J = 2.40 Hz, 1H), 7.85 (dd, J_1 = 8.65 Hz, J_2 = 2.52 Hz, 1H), 7.70 (d, J = 8.77 Hz, 1H) ppm; ^{13}C NMR (DMSO-d_6, 100 MHz) δ 160.31, 152.59, 146.45, 134.92, 131.49, 129.99, 125.31, 124.36 ppm; LC-MS 181.2 ([M+H]$^+$).

6-chloro-3-(2-oxopropyl)quinazolin-4(3H)-one (36):



To a solution of **32** (1.60 g, 6.76 mmol) in anhydrous NMP (15 mL) under nitrogen was added NaH (650 mg, 27.08 mmol) in small portions. The solution turned from a clear brown solution to a white precipitate. After stirring for 30 minutes, the solution returned to its clear brown state and chloroacetone (2.4 mL, 29.28 mmol) was added dropwise forming a deep red solution. The solution was concentrated in vacuo and recrystallized (3:1 hexane/ethyl acetate) yielding **36** (1.80 g, 86%) as a white needle crystal: R_f = 0.51 (100% EtOAc); ^{1}H NMR (DMSO-d_6, 400 MHz) δ 8.25 (s, 1H), 8.07 (d, J = 2.40 Hz, 1H), 7.89 (dd, J_1 = 8.73 Hz, J_2 = 2.48 Hz, 1H), 7.74 (d, J = 8.73 Hz, 1H), 4.98 (s, 2H), 2.25 (s, 3H) ppm; ^{13}C NMR ($CDCl_3$, 100 MHz) δ 199.7, 159.87, 146.7, 146.4, 135.0, 133.3, 129.3, 126.1, 122.9, 54.7, 27.5 ppm; LC-MS 237.1 ([M+H]$^+$).

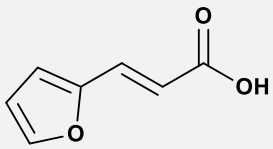
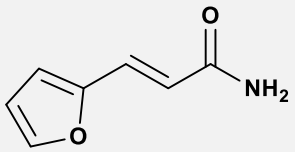
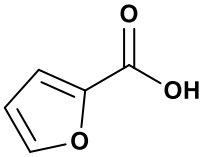
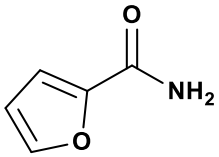
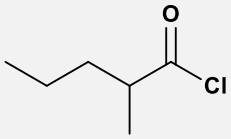
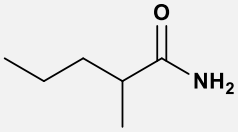
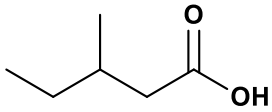
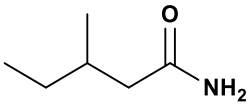
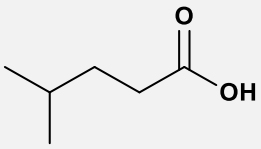
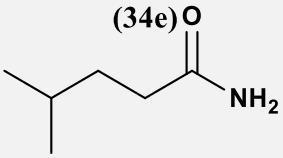
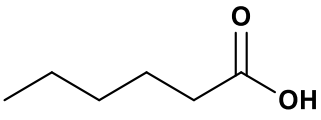
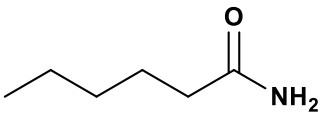
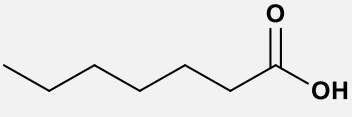
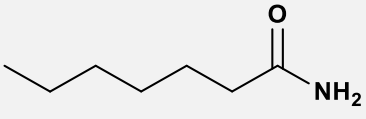
3-(3-bromo-2-oxopropyl)-6-chloroquinazolin-4(3H)-one (37):



To a solution of **36** (460 mg, 1.94 mmol) in acetic acid (10 mL) was added bromine (125 μL, 62.42 mmol) dropwise, forming a deep red solution. The reaction mixture was refluxed at 65 ^{o}C for 16 h, during which a red solid precipitated out, then cooled to room temperature. The mixture was concentrated in vacuo, dissolved in EtOAc and water and neutralized with 2 M NaOH. The mixture was washed with water (2 x 20 mL) and brine (1 x 20 mL) and the organic layer extracted with EtOAc (3 x 25 mL). The organic layers were combined and concentrated *in vacuo*. Purification through flash column chromatography (1:1 EtOAc/petroleum ether) yielded **36** (790 mg, 66%) as a white solid: R_f = 0.77 (100% EtOAc); ^{1}H NMR (DMSO-d_6, 400 MHz) δ 8.27 (s, 1H), 8.08 (d, J = 2.36 Hz, 1H), 7.90 (dd, J_1 = 8.69 Hz, J_2 = 2.40 Hz, 1H), 7.75 (d, J = 8.73 Hz, 1H), 5.13 (s, 2H), 4.57 (s, 2H) ppm; ^{13}C NMR ($CDCl_3$, 100 MHz) δ 194.6, 160.0, 146,7, 146.1, 135.2, 133.6, 129.5, 126.1, 122.8, 52.4, 31.4 ppm; LC-MS 315.1 ($[M+H]^+$).

General procedure for preparation of primary amides from carboxylic acids and acid chlorides

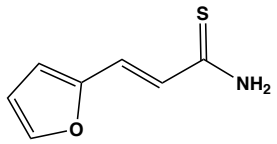
The appropriate carboxylic acid (1.72 mmol, 1 eq) and HATU (2.58 mmol, 1.5 eq) were dissolved in DMF (2 mL), NEt_3 (2 mL), NH_3 in MeOH (7N, 5 eq, 1 mL) and MeOH (3 mL). Upon the development of salt forming, the reaction mixture was sonicated until the salt was evenly dispersed throughout the solution and vigorous stirring was achieved. The reaction mixture was then stirred for 8 h at room temperature. The reaction mixture was diluted with EtOAc and water, neutralized with 2 M HCl and washed with water (3 x 20 mL) and brine (1 x 20 mL). The organic layer was then extracted with EtOAc (3 x 20 mL), the organic layers combined and concentrated in vacuo. Where acid chlorides were used, the process was identical except HATU was not introduced into the reaction mixture. The synthesized amides were carried through without purification.

Starting Material	Product
3-(Furan-2-yl)acrylic acid 	3-(Furan-2-yl)acrylamide (34a) 
Furan-2-carboxylic acid 	Furan-2-carboxamide (34b) 
2-Methylpentanoyl chloride 	2-Methylpentanamide (34c) 
3-Methylpentanoic acid 	3-Methylpentanamide (34d) 
4-Methylpentanoic acid 	4-Methylpentanamide (34e) 
Hexanoic acid 	Hexamide (34f) 
Heptanoic acid 	Heptamide (34g) 

General procedure for the preparation of thioamides

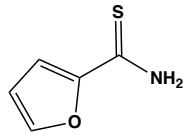
To a solution of the appropriate amide (1.72 mmol, 1 eq) in THF (5 mL) was added Lawesson's reagent (400 mg, 1.00 mmol, 0.57 eq) and the reaction stirred for 8 h at room temperature. Reaction of **34b → 35b** required heating to 40 °C. The reaction mixture was concentrated in vacuo and purified through flash column chromatography, with the exceptions of compounds **35l** which was recrystallised in 3:1 DCM/EtOAc. Prior to running the columns, the reaction mixture was left after loading for 1 h to age, allowing the Lawesson's reagent to decompose on silica. Chromatography was run in 1:2 → 1:1 EtOAc/petroleum ether → 100% EtOAc.

3-(Furan-2-yl)prop-2-enethioamide (35a):



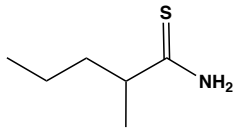
Obtained **35a** (126 mg, 38%) as a brown solid; ^{1}H NMR ($CDCl_3$, 400 MHz) δ 7.53-7.48 (m, 2H), 6.68 (dd, J_1 = 9.65 Hz, J_2 = 3.28, 1H), 6.49 (s, 1H), 6.32 (d, J = 15.65 Hz, 1H) ppm.

Furan-2-carbothioamide (35b):



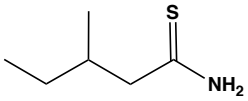
Obtained **35b** (97 mg, 44%) as a yellow crystal; ^{1}H NMR (DMSO-d_6, 400 MHz) δ 9.59 (br s, 1H), 9.28 (br s, 1H), 7.87 (d, J = 0.84 Hz, 1H), 7.24 (d, J = 3.48 Hz, 1H), 6.62 (dd, J_1 = 3.44 Hz, J_2 = 1.72Hz, 1H) ppm.

2-Methylpentanethioamide (35c):



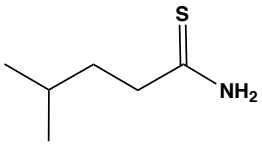
Obtained **35c** (150 mg, 66%) as a yellow solid; no proton NMR was obtained for **35c**.

3-Methylpentanethioamide (35d):



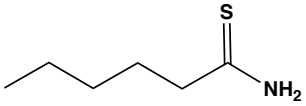
Obtained **35d** (53 mg, 24%) as a yellow crystal; ^{1}H NMR ($CDCl_3$, 400 MHz) δ 7.43 (br s, 1H), 6.78 (br s, 1H), 2.67 (dd, J_1 = 13.45 Hz, J_2 = 6.16 Hz, 1H), 2.41 (dd, J_1 = 13.45 Hz, J_2 = 8.41 Hz, 1H), 2.03 (qdd, $J_1 = J_2 = J_3$ = 6.69 Hz, 1H), 1.51-1.40 (m, 1H), 1.29-1.18 (m, 1H), 09.6 (d, J = 6.64 Hz, 3H), 0.92 (t, J = 7.41 Hz, 3H) ppm.

4-Methylpentanethioamide (35e):



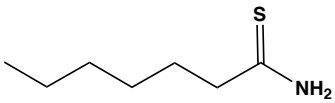
Obtained **35e** (125 mg, 55%) as a yellow solid; ^{1}H NMR ($CDCl_3$, 400 MHz) δ 7.55 (br s, 1H), 6.89 (br s, 1H), 2.68 (t, J = 7.41 Hz, 2H), 1.69-1.63 (m, 3H), 0.93 (d, J = 6.32 Hz, 6H) ppm.

Hexanethioamide (35f):



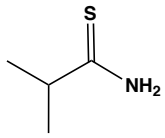
Obtained **35f** (182 mg, 80%) as a yellow oil; ^{1}H NMR ($CDCl_3$, 400 MHz) δ 7.52 (br s, 1H), 6.85 (br s, 1H), 2.68 (t, J = 7.77 Hz, 2H), 1.77 (tt, $J_1 = J_2$ = 7.65 Hz, 2H), 1.36-1.33 (m, 4H), 0.90 (t, J = 7.08 Hz, 3H) ppm.

Heptanethioamide (35g):



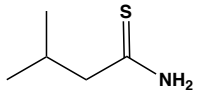
Obtained **35g** (150 mg, 42%), as a yellow solid; no proton NMR was obtained for **35g**.

2-Methylpropanethioamide (35h):



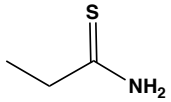
Obtained **35h** (91 mg, 51%) as a yellow crystal; ^{1}H NMR (DMSO-d_6, 400 MHz) δ 9.30 (br s, 1H), 9.07 (br s, 1H), 2.78 (qq, $J_1 = J_2$ = 6.76 Hz, 1H), 1.08 (d, J = 6.72 Hz, 6H) ppm.

3-Methylbutanethioamide (35i):



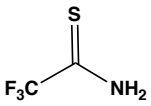
Obtained **35i** (127 mg, 63%) as a yellow crystal; ^{1}H NMR (DMSO-d_6, 400 MHz) δ 9.33 (br s, 1H), 9.10 (br s, 1H), 2.32 (d, J = 7.28, 2H), (qt, $J_1 = J_2$ = 6.89 Hz, 1H), 0.88 (d, J = 6.64 Hz, 6H) ppm.

Propanethioamide (35j):



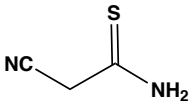
Obtained **35j** (113 mg, 74%) as a yellow crystal; ^{1}H NMR (DMSO-d_6, 400 MHz) δ 9.31 (br s, 1H), 9.11 (br s, 1H), 2.46 (q, J = 7.52 Hz, 2H), 1.14 (t, J = 7.56 Hz, 3H) ppm.

2,2,2-Trifluoroehtanethioamide (35k):



Obtained **35k** (75 mg, 34%) as a yellow solid; no analysis was undertaken for **8l** due to the lack of protons, with the exception of the thioamide-protons.

2-Cyanoethanethioamide (35l):

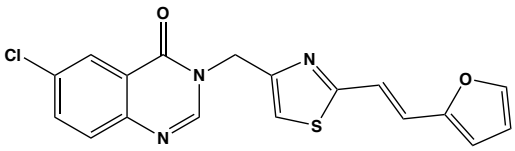


Obtained **35l** (34 mg, 14%) as white needle crystals; ^{1}H NMR ($CDCl_3$, 400 MHz) δ 7.60 (br s, 1H), 7.38 (br s, 1H), 3.92 (s, 2H) ppm.

General procedure for the preparation of thiazoles

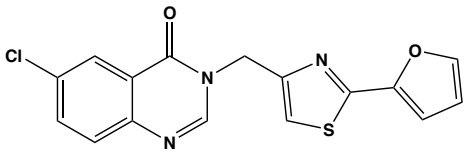
A solution of the appropriate thioamide (0.13 mmol, 2 eq) and 3 (20 mg, 0.06 mmol) in EtOH (10 mL) was refluxed at 80 ^{o}C for 16 h. After cooling to room temperature, the reaction mixture was concentrated in vacuo and purified through flash column chromatography. Chromatography was run in 1:2 → 1:1 EtOAc/petroleum ether → 100% EtOAc with the exceptions of compounds **31l** and **31p** which were run in 19:1 DCM/MeOH and 9:1 DCM/MeOH respectively. All R_f values were determined in 3:1 EtOAc/petroleum ether. In cases where ^{13}C NMR data is missing, either too little compound was synthesized for an accurate run or solubility issues prevented a clear spectrum from forming. In the case of **31a**, many of the minor product's ^{1}H NMR peaks were unclear, so only the key peaks were included. Furthermore, the peaks of **31a**'s ^{13}NMR spectrum could not be distinguished, so were reported together.

6-Chloro-3-((2-(2-(furan-2-yl)vinyl)thiazol-4-yl)methyl)quinazolin-4(3H)-one (31a):



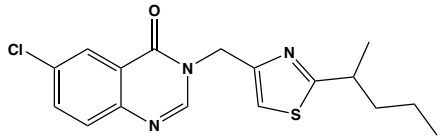
Obtained **31a** (12 mg, 51%) as a cream solid. Upon ^{1}H NMR analysis, the product was shown to contain two isomers in a ratio 5:1: R_f = 0.65, 0.76; ^{1}H NMR (DMSO-d_6, 400 MHz, major product) δ 8.60 (s, 1H), 8.09 (d, J = 2.32 Hz, 1H), 7.88 (dd, J_1 = 8.73 Hz, J_2 = 2.36 Hz, 1H), 7.77-7.73 (m, 2H), 7.54 (s, 1H), 7.29 (d, J = 16.09 Hz, 1H), 7.08 (d, J = 16.09 Hz, 1H), 6.79 (d, J = 3.24 Hz, 1H), 6.59 (dd, J_1 = 2.88 Hz, J_2 = 1.64 Hz, 1H), 5.30 (s, 2H) ppm; ^{1}H NMR (DMSO-d_6, 400 MHz, minor product) δ 7.39 (d, J = 15.77 Hz, 1H), 6.93 (d, J = 3.32 Hz, 1H), 6.63 (m, 1H), 6.17 (d, J = 15.85 Hz, 1H); ^{13}C NMR (DMSO-d_6 100 MHz) δ 167.3, 166.0, 159.0, 151.6, 151.1, 150.3, 148.6, 146.7, 146.7, 144.5, 134.6, 131.4, 130.8, 128.6, 125.1, 122.9, 121.4, 118.3, 116.9, 116.0, 115.4, 112.7, 112.5, 45.5 ppm; LC-MS 370.2 ($[M+H]^+$).

6-Chloro-3-((2-(furan-2-yl)thiazol-4-yl)methyl)quinazolin-4(3H)-one (31b):



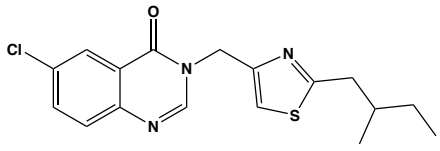
Obtained **31b** (17.4 mg, 80%) as a white crystal: $R_f = 0.82$; ^{1}H NMR ($CDCl_3$, 400 MHz) δ 8.40 (s, 1H), 8.26 (d, $J = 1.88$ Hz, 1H), 7.67 (d, $J = 2.20$ Hz, 1H), 7.66 (s, 1H), 7.50 (d, $J = 1.09$ Hz, 1H), 7.32 (s, 1H), 6.97 (d, $J = 3.64$ Hz, 1H), 6.52 (dd, $J_1 = 3.36$ Hz, $J_2 = 1.80$ Hz, 1H), 5.29 (s, 2H) ppm; ^{13}C NMR ($CDCl_3$ 100 MHz) δ 159.9, 158.9, 150.6, 148.5, 146.9, 146.6, 143.9, 134.8, 133.2, 129.2, 126.2, 123.2, 117.3, 112.3, 109.5, 45.4 ppm; LC-MS 344.1 ($[M+H]^+$).

6-Chloro-3-((2-(pentan-2-yl)thiazol-4-yl)methyl)quinazolin-4(3H)-one (31c):



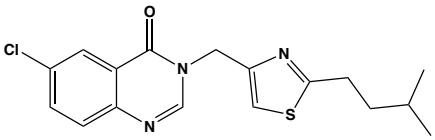
Obtained **31c** (11.3 mg, 45%) as a yellow oily solid: $R_f = 0$ .76; ^{1}H NMR ($CDCl_3$, 400 MHz) δ 8.37 (s, 1H), 8.25 (d, $J = 1.52$ Hz, 1H), 7.69-7.63 (m, 2H), 7.20 (s, 1H), 5.24 (s, 2H), 3.14 (qt, $J_1 = J_2 = 6.96$ Hz, 1H), 1.77-1.53 (m, 2H), 1.33-1.25 (m, 5H), 0.88 (t, $J = 7.32$ Hz, 3H) ppm; ^{13}C NMR ($CDCl_3$ 100 MHz) δ 178.6, 159.8, 148.8, 147.0, 146.5, 134.7, 133.1, 129.1, 126.2, 123.2, 116.7, 45.3, 39.9, 38.3, 21.4, 20.3, 13.9 ppm; LC-MS 348.2 ($[M+H]^+$).

6-Chloro-3-((2-(2-methylbutyl)thiazol-4-yl)methyl)quinazolin-4(3H)-one (31d):



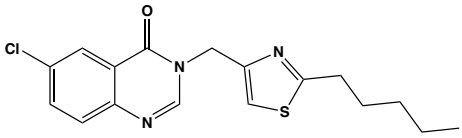
Obtained **31d** (20 mg, 91%) as a colourless oil: $R_f = 0$ .76; ^{1}H NMR ($CDCl_3$, 400 MHz) δ 8.35 (s, 1H), 8.25 (d, $J = 1.64$ Hz, 1H), 7.69-7.63 (m, 2H), 7.21 (s, 1H), 5.24 (s, 2H), 2.94 (dd, $J_1 = 14.61$ Hz, $J_2 = 6.08$ Hz, 1H), 2.75 (dd, $J_1 = 14.61$ Hz, $J_2 = 8.09$, 1H), 1.89-1.80 (m, 1H), 1.46-1.14 (m, 2H), 0.92-0.87 (m, 6H) ppm; ^{13}C NMR ($CDCl_3$ 100 MHz) δ 171.6, 159.7, 149.2, 146.9, 146.6, 134.7, 129.2, 126.2, 123.0, 117.3, 45.4, 40.3, 36.0, 29.7, 29.1, 19.0, 11.3 ppm; LC-MS 348.2 ($[M+H]^+$).

6-Chloro-3-((2-isopentylthiazol-4-yl)methyl)quinazolin-4(3H)-one (31e):



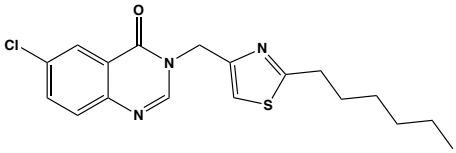
Obtained **31e** (13.5 mg, 71%) as a white crystal: R_f = 0 .76; ^{1}H NMR ($CDCl_3$, 400 MHz) δ 8.36 (s, 1H), 8.25 (d, *J* = 1.48 Hz, 1H), 7.69-7.63 (m, 2H), 7.20 (s, 1H), 5.23 (s, 2H), 2.95 (t, *J* = 7.61 Hz, 2H), 1.65-1.62 (m, 3H), 0.93 (d, *J* = 6.04 Hz, 6H); ^{13}C NMR ($CDCl_3$ 100 MHz) δ 172.9, 159.8, 149.2, 146.9, 134.7, 133.0, 129.2, 126.2, 123.3, 117.2, 45.4, 38.9, 31.5, 29.7, 27.7, 23.3 ppm; LC-MS 348.2 ($[M+H]^+$).

6-Chloro-3-((2-pentylthiazol-4-yl)methyl)quinazolin-4(3H)-one (31f):



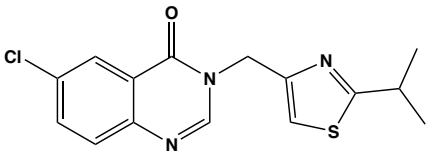
Obtained **31f** (20 mg, 90%) as a white crystal R_f = 0 .82; ^{1}H NMR ($CDCl_3$, 400 MHz) δ 8.35 (s, 1H), 8.26 (d, *J* = 1.92 Hz, 1H), 7.69-7.63 (m, 2H), 7.20 (s, 1H), 5.23 (s, 2H), 2.93 (t, *J* = 7.68 Hz, 2H), 1.77-1.69 (m, 2H), 1.37-1.33 (m, 4H), 0.90 (t, *J* = 6.93 Hz, 3H) ppm; LC-MS 348.2 ($[M+H]^+$).

6-Chloro-3-((2-hexylthiazol-4-yl)methyl)quinazolin-4(3H)-one (31g):



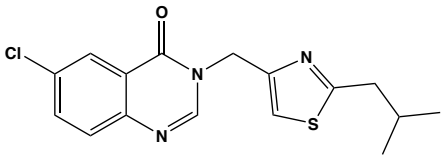
Obtained **31g** (15 mg, 66%) as a white crystal: R_f = 0.85; ^{1}H NMR ($CDCl_3$, 400 MHz) δ 8.36 (s, 1H), 8.25 (d, *J* = 1.72 Hz, 1H), 7.69-7.64 (m, 2H), 7.21 (s, 1H), 5.23 (s, 2H), 2.94 (t, *J* = 7.89 Hz, 2H), 1.74 (tt, $J_1 = J_2$ = 7.64 Hz, 2H), 1.40-1.33 (m, 2H), 1.30-1.27 (m, 4H), 0.86 (t, *J* = 6.93 Hz, 3H) ppm; ^{13}C NMR ($CDCl_3$ 100 MHz) δ 172.8, 159.8, 149.1, 146.9, 146.5, 134.7, 133.1, 129.1, 126.1, 123.2, 117.2, 45.4, 33.4, 31.4, 29.9, 28.7, 22.4, 14.0 ppm; LC-MS 362.3 ($[M+H]^+$).

6-Chloro-3-((2-isopropylthiazol-4-yl)methyl)quinazolin-4(3H)-one (31h):



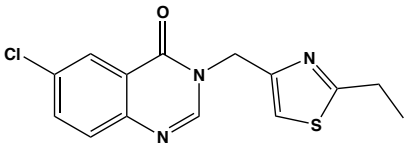
Obtained **31h** (18.4 mg, 90%) as a white crystal: R_f = 0 .71; ^{1}H NMR (DMSO-d_6, 400 MHz) δ 8.54 (s, 1H), 8.05 (d, J = 1.68 Hz, 1H), 7.83 (dd, J_1 = 8.61 Hz, J_2 = 1.72 Hz, 1H), 7.70 (d, J = 8.69 Hz, 1H), 7.39 (s, 1H), 5.25 (s, 2H), 3.24-3.17 (m, 1H), 1.26 (d, J = 6.84 Hz, 6H) ppm; ^{13}C NMR (DMSO-d_6 100 MHz) δ 177.7, 158.9, 150.0, 148.5, 146.6, 134.5, 131.4, 129.5, 125.1, 122.9, 115.7, 45.4, 32.4, 22.8 ppm; LC-MS 320.1 ([M+H]$^+$).

6-Chloro-3-((2-isobutylthiazol-4-yl)methyl)quinazolin-4(3H)-one (31i):



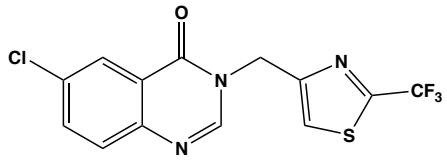
Obtained **31i** (11 mg, 53%) as a silver crystal: R_f = 0 .72; ^{1}H NMR (DMSO-d_6, 400 MHz) δ 8.54 (s, 1H), 8.07 (d, J = 2.36 Hz, 1H), 7.86 (dd, J_1 = 8.69 Hz, J_2 = 2.40 Hz, 1H), 7.72 (d, J = 8.69 Hz, 1H), 7.42 (s, 1H), 5.25 (s, 2H), 2.77 (d, J = 7.08 Hz, 2H), 1.95 (qt, J_1 = J_2 = 6.72 Hz, 1H), 0.88 (d, J = 6.65 Hz, 6H) ppm; ^{13}C NMR (DMSO-d_6, 100 MHz) δ 170.1, 158.9, 150.1, 148.6, 146.6, 134.5, 131.4, 129.5, 125.1, 122.9, 116.4, 45.3, 41.2, 29.1, 21.9 ppm; LC-MS 334.1 ([M+H]$^+$).

6-Chloro-3-((2-ethylthiazol-4-yl)methyl)quinazolin-4(3H)-one (31j):



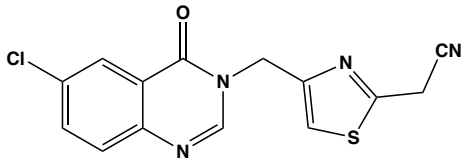
Obtained **31j** (14 mg, 70%) as a white solid: R_f = 0 .76; ^{1}H NMR ($CDCl_3$, 400 MHz) δ 8.28 (s, 1H), 8.15 (s, 1H), 7.61-7.55 (m, 2H), 7.14 (s, 1H), 5.16 (s 2H), 2.90 (q, J = 7.52 Hz, 2H), 1.27 (t, J = 7.56 Hz, 3H) ppm; ^{13}C NMR ($CDCl_3$ 100 MHz) δ 173.9, 159.7, 149.1, 147.0, 146.5, 134.6, 132.9, 129.1, 126.0, 123.1, 117.1, 45.3, 26.8, 14.0 ppm; LC-MS 306.1 ([M+H]$^+$).

6-Chloro-3-((2-(trifluoromethyl)thiazol-4-yl)methyl)quinazolin-4(3H)-one (31k):



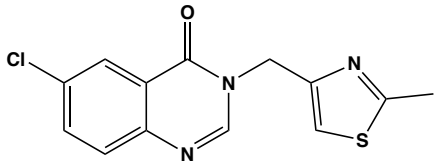
Obtained **31k** (3.5 mg, 16%) as a yellow solid: R_f = 0 .81; ^{1}H NMR ($CDCl_3$, 400 MHz) δ 8.35 (s, 1H), 8.24 (d, *J* = 1.64 Hz, 1H), 7.71 (s, 1H), 7.69-7.66 (m, 2H), 5.32 (s, 2H) ppm; LC-MS 346.1 ($[M+H]^+$).

2-(4-((6-Chloro-4-oxoquinazolin-3(4H)-yl)methyl)thiazol-2-yl)acetonitrile (31l):



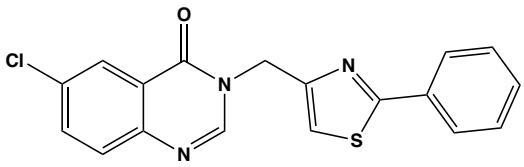
Obtained **31l** (18 mg, 90%) as a red-orange solid: R_f = 0 .47; ^{1}H NMR ($CDCl_3$, 400 MHz) δ 8.32 (s, 1H), 8.23 (d, *J* = 1.80 Hz, 1H), 7.70-7.64 (m, 2H), 7.43 (s, 1H), 5.24 (s, 2H), 4.06 (s, 2H) ppm; ^{13}C NMR ($CDCl_3$ 100 MHz) δ 159.8, 158.4, 150.6, 146.6, 146.5, 134.8, 133.3, 129.2, 126.1, 123.1, 119.8, 115.0, 45.3, 22.2 ppm; LC-MS 317.2 ($[M+H]^+$).

6-Chloro-3-((2-methylthiazol-4-yl)methyl)quinazolin-4(3H)-one (31m):



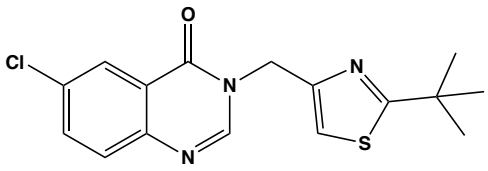
Obtained **31m** (17 mg, 90%) as an orange crystal: R_f = 0 .76; ^{1}H NMR ($CDCl_3$, 400 MHz) δ 8.34 (s, 1H), 8.25 (d, *J* = 1.24 Hz, 1H), 7.69-7.63 (m, 2H), 7.20 (s, 1H), 5.22 (s, 2H), 2.66 (s, 3H) ppm; ^{13}C NMR ($CDCl_3$ 100 MHz) δ 159.9, 149.4, 146.9, 146.6, 134.7, 133.1, 129.2, 126.2, 123.2, 117.7, 45.4, 29.7, 19.1 ppm; LC-MS 292.1 ($[M+H]^+$).

6-Chloro-3-((2-phenylthiazol-4-yl)methyl)quinazolin-4(3H)-one (31n):



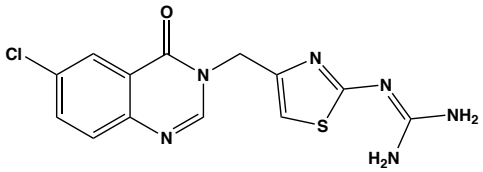
Obtained **31n** (20 mg, 89%) as a white solid: R_f = 0.85; ^{1}H NMR ($CDCl_3$, 400 MHz) δ 8.47 (s, 1H), 8.27 (d, *J* = 1.72 Hz, 1H), 7.92-7.89 (m, 2H), 7.70-7.64 (m, 2H), 7.43-7.41 (m, 3H), 7.36 (s, 1H), 5.32 (s, 2H) ppm; LC-MS 354.2 ($[M+H]^+$).

3-**((2-(Tert-butyl)thiazol-4-yl)methyl)-6-chloroquinazolin-4(3H)-one (31o):**



Obtained **31o** (2.5 mg, 12%) as a white crystal: R_f = 0 .85; ^{1}H NMR ($CDCl_3$, 400 MHz) δ 8.43 (s, 1H), 8.27 (d, *J* = 1.80 Hz, 1H), 7.70-7.65 (m, 2H), 7.19 (s, 1H), 5.26 (s, 2H), 1.40 (s, 9H) ppm; LC-MS 334.2 ($[M+H]^+$).

2-(4-((6-Chloro-4-oxoquinazolin-3(4H)-yl)methyl)thiazol-2-yl)guanidine (31p):



Obtained **31p** (13 mg, 62%) as a cream solid: R_f = 0 (baseline); ^{1}H NMR (DMSO-d_6, 400 MHz) δ 8.55 (s, 1H), 8.08 (d, *J* = 2.40 Hz, 1H), 7.85-7.83 (m, 1H), 7.70 (dd, J_1 = 8.77 Hz, J_2 = 2.36 Hz, 1H), 7.04 (br s, 4H), 5.06 (s, 2H) ppm; LC-MS 335.2 ($[M+H]^+$).